Study of Occupant Model Capability to Quantify Injury Risk for eVTOL Vehicles

Nathaniel Levi Jones

Thesis submitted to the faculty of the Virginia Polytechnic Institute and State University in partial fulfillment of the requirements for the degree of

Master of Science

In

Biomedical Engineering

Costin D. Untaroiu, Chair

Christopher B. Arena

Miguel A. Perez

February 4, 2025

Blacksburg, VA

Keywords: occupant safety, finite element modeling, aerospace impact

Study of Occupant Model Capability to Quantify Injury Risk for eVTOL Vehicles

Nathaniel Levi Jones

ABSTRACT

Urban transportation is evolving from traditional ground-based vehicles (e.g., cars, taxis, and buses) to air-based electric vertical take-off and landing (eVTOL) vehicles, which can be utilized for on-demand transportation, cargo transport, and emergency services. These new eVTOL vehicles are designed to be manoeuvrable, lightweight, and autonomously operable without user intervention. Safety is a big part of eventual eVTOL adoption; however, gaps in safety features exist. Anthropomorphic test devices (ATDs) are used in aerospace crashworthiness standards to quantify occupant injury risk and develop improved safety designs for emergency landing situations despite their development many decades ago. ATD technology has continued to evolve, leading to newer and more biofield ATDs, such as the Test Device for Human Occupant Restraint (THOR). Increased computing power has also created detailed computational human body models (HBMs), such as the Global Human Body Model Consortium (GHBMC). This study aims to assess the capability of both HBMs and new ATD designs to identify injury mechanisms within eVTOL-relevant emergency landing conditions.

Before HBMs to be used in eVTOL crash simulation, they had to be tested in airspace crash environment. Researchers at The National Aeronautics and Space Administration (NASA) Langley Research Center (LaRC) previously conducted a full-scale crash test of a Fokker F28 MK1000 aircraft to study occupant injury risks. The goal of the current study was to investigate

the injury predictions of the Global Human Body Models Consortium (GHBMC) and Total Human Model for Safety (THUMS) occupant models in the tested aircraft crash condition and explore possible utilization of human body models (HBMs) in this context. Eight crash conditions were simulated utilizing each of the models. The HBMs were positioned in two postures: a neutral, upright posture with hands resting on the legs and feet contacting the floor and a braced posture with head and hand contact with the forward seat back. Head and Neck injury metrics and Lumbar Vertebra axial force were calculated and compared for all simulations. Two HBMs reported similar kinematic responses in the simulated impact conditions. However, the GHBMC model reported higher forces and injury risks in almost all scenarios. The HBMs were compared to responses from previously modeled anthropomorphic test devices (ATD). The HBMs showed higher loading than the modeled ATDs in two of eight impact conditions. Relative to the THUMS model, the GHBMC model included more virtual instrumentation and produced injury metric values, encompassing the THUMS model. The THUMS model has additional value in being a free-access model. Both models provided valuable insight into the potential response of the human body within the simulated aerospace crash environment.

Then, finite element (FE) analysis was used to expand upon eVTOL full-scale and seat-level impact testing conducted by researchers at the National Aeronautics and Space Administration (NASA) to examine the effects of occupant model configurations on injury prediction. The GHBMC HBM and THOR ATD models were simulated in seat-level test conditions to characterize differences between these advanced assessment tools and

traditional ATDs in the isolated seat-loading environment. Of these test conditions, four crash pulses were implemented to a rigid seat, with two being implemented in a generic composite seat and a NASA-designed energy-absorbing seat. Further exploration was performed by altering the position of the GHBMC into a relaxed and upright position. Results compared the impact response in head, neck, and spinal injury metrics and identified key differences in the responses from each model. The GHBMC showed distinctly different biomechanical reactions compared to the ATD. As expected, the GHBMC models were much more deformable than the ATDs, exhibited a higher distribution of forces, and increased sensitivity to the duration of acceleration pulses. Both occupant models incorporated into this study identified key mechanisms for injury that should be considered for passenger safety in developing these novel aircraft. In addition, this study demonstrated the value of FE modelling for running a variety of complex human surrogates to identify potential injury mechanisms for consideration in the regulation and development of new aircraft. Continued research in this field to improve the validation of these models will only lead to safer aircraft and more comprehensive safety measures.

Study of Occupant Model Capability to Quantify Injury Risk for eVTOL Vehicles

Nathaniel Levi Jones

GENERAL AUDIENCE ABSTRACT

Technological developments are leading the aerospace industry into a new era of aircraft design. Advancements in electric motors and batteries are allowing for the development of electric Vertical Take-off and Landing vehicles (eVTOLs). These aircraft are being developed by many of the world's leading automotive and aerospace manufacturers. These new aircraft will need extensive testing and research to ensure passengers' safety and allow eventual adoption. However, physical testing of vehicles of this sort can be costly and time-consuming. Finite Element Modelling (FEM) is a technique that enables researchers to create computer simulations to predict potential injuries in crash events. This study implemented advanced occupant models in passenger aircraft and potential eVTOL aircraft simulations. This research compared these models to physical test data to analyse the capability of this technology for utilization in future testing. In addition, this study identified potential injury mechanisms reported by two FE human models.

Acknowledgments

First, I'd like to thank my advisor, Costin Untaroiu, for encouraging me to stick with my research and complete a master's degree. His encouragement and, at times, harsh feedback have made me a better writer and researcher. In addition, Daniel Grindle was invaluable in my initial introduction to FEM modeling, and his mentorship and teaching helped me become the researcher I am today.

I would also like to thank Jacob Putnam and NASA Langley Research Center for sponsoring the project and my master's degree. Without them, I would never have done such interesting research and obtained a master's in biomedical engineering.

To my friends and family, their undying support throughout my entire journey as an undergrad and master's student was key to allowing me to persevere and complete the master's requirements.

Finally, thank you to the rest of my master's board and all the excellent instructors I have had throughout my time at Virginia Tech. Every course at Tech has fueled my thirst for knowledge and my love for biomedical engineering.

Attributions

Several colleagues aided in the writing and research behind the chapters presented as part of this thesis. A brief description of their contribution is included here.

Chapter 2: Evaluation of Occupant Injury Risk in a Transport Aircraft Crash Test Environment: Accepted for publication in SAE International Journal of Commercial Vehicles.

Costin D. Untaroiu, (Center for Injury Biomechanics, Department of Biomedical Engineering and Mechanics), is an associate professor of biomedical engineering and mechanics at Virginia Tech. Dr. Untaroiu was a co-author on this paper, investigator for the contracts supporting the research, and contributed editorial comments.

Putnam, Jacob, (NASA Langley Research Center) is an aerospace research engineer out of NASA Langley Research Center. Mr. Putnam was a co-author on this paper and was a point of contact providing physical test data and simulation environments.

Chapter 3: Study of Advanced Occupant Models to Quantify Injury Risk for eVTOL Vehicles: Accepted for publication in the Journal of American Helicopter Safety.

Costin D. Untaroiu, (Center for Injury Biomechanics, Department of Biomedical Engineering and Mechanics), is an associate professor of biomedical engineering and mechanics at Virginia Tech. Dr. Untaroiu was a co-author on this paper, investigator for the contracts supporting the research, and contributed editorial comments.

Putnam, Jacob, (NASA Langley Research Center) is an aerospace research engineer out of NASA Langley Research Center. Mr. Putnam was a co-author on this paper and was a point of contact providing physical test data and simulation environments.

Table of Contents

List of Figures

List of Tables

Chapter 1: Introduction and Background

The burgeoning electric Vertical Take-Off and Landing (eVTOL) vehicles for the aviation industry have generated significant enthusiasm among aviation designers, manufacturers, researchers, and consumers. This industry is determined to change the urban transportation paradigm from traditional ground-based vehicles (e.g., cars, taxis, buses) to air-based eVTOL vehicles, which can be utilized for on-demand transportation, cargo transport, and emergency services. These new eVTOL vehicles are designed to be minor, lightweight, and able to operate autonomously without user intervention. Safety is a big part of eventual eVTOL adoption. However, gaps in addressing the considerations of safety features exist. These studies, supported and funded by NASA, will focus on the safety characteristics of eVTOL vehicles within the urban air market as they pertain to the protection of the occupants in emergency landing situations. A high level of safety is necessary for these vehicles to gain the level of public acceptance required to become a new daily form of transportation, and standards organizations need data to set safety standards.

The Anthropomorphic Test Device (ATD) is currently used in aerospace crashworthiness standards to quantify occupant injury risk and develop improved safety designs for emergency landing situations. The ATDs presently used in aircraft certification requirements were created more than 40 years ago, and the hardware has been essentially unchanged since its initial development [11]. Significant developments have occurred over the years involving ATD technology, including newer and higher biofield ATDs, such as the Test Device for Human Occupant Restraint (THOR) [14]. Increased computing power has also allowed for detailed

computational human body models (HBMs) to be created, such as the Global Human Body Model Consortium (GHBMC) and Total Human Model for Safety (THUMS) [16,19]. These models offer promise to predict human injury risk more accurately in the crash environment because of their fidelity in detailed capturing of the human body and because the models are inherently more biomimetic than ATDs. These HBMs have been evaluated for automotive environments; however, their capability to predict injury within aircraft loading environments has yet to be quantified.

Crashworthiness and Aircraft Safety:

Crashworthiness is the ability of a vehicle to protect its occupants or cargo during an impact event [1]. This ability of any vehicle is a key attribute for consideration in any vehicle design. Federal regulations focus on crashworthiness and vehicle safety as a key factors in regulating aircraft design [2]. Researchers have analyzed the development and improvement of aircraft crashworthiness for over half a century. Studies as early as 1975 have identified crashworthiness as a key component in occupant safety. However, even in these early studies, many fatal and serious injuries occurred due to unsatisfactory seat/restraint systems in low-velocity impacts [3]. Aviation accidents continue to reduce in frequency, with the National Transportation Safety Board (NTSB) reporting a reduction from 3593 crashes in 1982 to 1581 reported in 2018 [4]. However, the NTSB also noted that the average number of fatal injuries per crash event, 0.44 in 1982 and 0.54 in 2018, had increased. While a multitude of factors contribute to these changes in statistics, including larger aircraft size, the data alludes that

further improvements in the crashworthiness of aircraft may be necessary to improve crash safety.

Current aircraft designs undergo extensive testing to ensure crashworthiness. The overall goal of these tests is to reduce the impact load transmitted to the occupant. These loads are transmitted through the sub-cargo floor support struts, cargo cross beam, fuselage frame, cabin floor support struts, and passenger cross beam, and finally transmitted through the seats to the occupant [5]. Designers can significantly improve crashworthiness using energy-absorbing materials and structures [6]. Many aircraft undergo the "building block approach of crashworthiness." This approach applies a multileveled approach to test materials, subcomponents, components, and full-scale aircraft [7]. While the subcomponent and component level tests provide valuable data for improving aircraft design, full-scale crash testing is the most comprehensive.

Testing and evaluation:

The leading method for testing and evaluation of crashworthiness is full-scale impact testing. These tests can be expensive, and while there isn't extensive data on the cost of aircraft tests, automotive full-scale tests cost around $50,000 per test [8]. Intuitively, aerospace full-scale tests can be even more expensive due to the higher number of ATDs required and vehicle and facility costs. In addition, these tests can take months to years to get the proper approvals and resources to run. A helpful tool to alleviate some of the limitations of full-scale testing is finite element (FE) modeling.

Finite element modeling is a technique that utilizes math to break down complex systems into more minor elements. By applying differential equations to each component, computers can simulate the physical responses of complex physical interactions without the expense and time of physical testing [9]. Over two decades ago, NASA began utilizing FE modeling, specifically the LS-Dyna software, to develop aircraft models for crash simulations [10]. These simulations were compared to physical test data, and high correlations were seen between predicted and tested damage in vertical impact scenarios. In addition to modeling fuselage response, researchers began to develop and utilize FE models of ATDs to investigate injury biomechanics within impact environments. Using FE modeling allows researchers to efficiently research the implementation of new composite materials and aircraft designs without the associated costs of extensive physical testing.

Occupants:

In both physical testing and FE simulations, a multitude of occupant surrogates are utilized to evaluate injury biomechanics. The most accurate surrogate is a postmortem human surrogate (PMHS); however, PMHSs are both expensive and challenging. The most widely utilized nonhuman occupants for physical tests are ATD crash test dummies. There are various leading ATD dummies, but one of the most utilized is the Hybrid III crash test dummy.

The Hybrid III was initially developed over 40 years ago for automotive crash research by General Motors [11]. The Hybrid III dummy underwent lumbar spinal modifications to build the Hybrid III FAA dummy for the specific use of aircraft seat testing [12]. While these dummies are useful in investigations of aircraft safety, some studies have identified injuries in humans

not reported by ATD testing [13]. These discoveries identified a need for more advanced dummies such as the THOR ATD.

The Test Device for Occupant Restraint (THOR) crash test dummy was developed by the National Highway Traffic Safety Administration in 1982. Comparisons between the THOR and Hybrid III in automotive sled testing identified differences in responses, including lower shear, axial force, and lateral moment in the THOR spine [14]. While the THOR model was more complex than previous ATDs, the THOR response was not necessarily deemed more or less accurate than the Hybrid III model. While Hybrid III and THOR have been modified and utilized in aerospace environments, neither was initially developed for this purpose.

The first dummy directly developed for vertical loading was the WIAMan Blast dummy developed by the U.S. ARMY [15]. This dummy was explicitly designed to investigate underbody blast loading and, in turn, is a valuable tool for examining aviation crash events.

These physical dummies have been developed into FE models to recreate and simulate physical tests. However, using FE modeling also allows for creating and utilizing advanced human body models. These complex FE models have been validated against PMHS data to best represent the human body in simulated crash tests [16-18]. Two of these widely used models include the Global Human Body Models Consortium (GHBMC) [16] and the Total Human Model for Safety (THUMS)[19]. These models have been extensively validated in various automotive loading scenarios [16,19]. They are used to predict human injury risk during impact; however, their capability to predict injury within aircraft loading environments has not been extensively studied.

Each occupant surrogate has benefits and drawbacks for aerospace research. The ATDs are the cheapest and most repeatable options for use in physical testing. However, their rigid constructions for repeatability may come at the cost of infidelity. HBMs are a complex and novel approach; however, they are difficult to validate in simulations without connected PMHS data. A combination of techniques is the best way to evaluate the current state of both physical testing and FE modeling to identify current gaps and potentials for all investigative methods.

eVTOL Development:

Electric Vertical take-off and landing (VTOL) aircraft are a promising new development in air transport. Over 150 companies are in the process of developing prototypes of this new technology [20]. These vehicles are designed to expand urban transportation from ground-based to the sky. EVTOLs would also allow for efficient transport of cargo, people, and emergency services. These aircraft are designed to be small and lightweight to benefit mobility and efficiency. In addition, many eVTOL designs allow the vehicles to operate as combination aircraft with vertical takeoff capability, transitioning to a more standard gliding aircraft upon clearing potentially constrained takeoff and landing zones. These unique features create new loading conditions in emergency landing situations that may necessitate novel safety features for passengers.

There are multiple leading configurations being developed for eVTOL vehicles. The first of three emerging designs is a multi-rotor aircraft. Similar to designs seen in hobby drones, these aircraft have multiple electric motors that allow for controlled flight. Another design is

lift + cruise type eVTOLs. These eVTOLs allow for vertical landing and takeoff. However, they also have fixed wings, allowing extended cruising in open airways [21]. Finally, vectored thrust eVTOLS utilize similar systems for lift and cruise. However, they can orient the thrust direction, providing flexible aerodynamic control [22]. All three leading aircraft types rely on lightweight composite materials for energy efficiency. These lightweight composite materials, in addition to the aircraft's novel designs, necessitate crashworthiness research to aid in developing and regulating these aircraft.

Objectives:

This current study expands on work performed by NASA Langley Research Center researchers. These researchers utilized a full-scale passenger aircraft test to develop a Finite Element (FE) breakout model to investigate injury levels and mechanisms utilizing simulated recreations of the crash. In addition, they performed seat testing and a full-scale drop test of a novel eVTOL aircraft shell design. The present research aimed to implement advanced ATD and HBMs into the simulation environments to compare the reported injury risks and mechanisms. This work was achieved through the following aims:

1. Implement advanced HBMs into a realistic passenger aircraft simulation to identify the capability of the HBMs for use in aerospace environments.
2. Utilize HBMs and advanced ATD models to compare to tested eVTOL seat tests.
3. Implement a HBM into a realistic eVTOL crash simulation.

The primary objective of this study was to assess the capability of advanced models in their implementation in these complex aerospace crash environments. This was done by

comparing injury metric outputs from the advanced models against physical test data. In addition, this study identified potential future work needed to expand the utilization of HBMs for aerospace crashworthiness assessments.

Chapter 2: Evaluation of Occupant Injury Risk in a Transport Aircraft Crash Test Environment

Introduction:

Transport category aircraft (TCA), as defined by 14 Code of Federal Regulations (CFR) Part 25, have been utilized to transport people around the world for almost 100 years [2]. These aircraft, which were first developed in the early 1900s, have evolved into high-tech, ultra-efficient airplanes that now use advanced materials such as composites for their construction. Along with the development of flight technology, the goal of occupant safety is a key factor in improving the future of aviation.

Researchers at the National Aeronautics and Space Administration (NASA) Langley Research Center (LaRC) have conducted a full-scale crash test of a Fokker F28 MK1000 aircraft to study occupant injury risks in TCA [23]. Twenty-four Anthropomorphic Test Devices (ATDs) were used in this test as surrogate occupants. In addition, the researchers at NASA LaRC computationally recreated the physical crash environment utilizing finite element (FE) modeling

to study occupant injury risk further [24] (Figure 1).

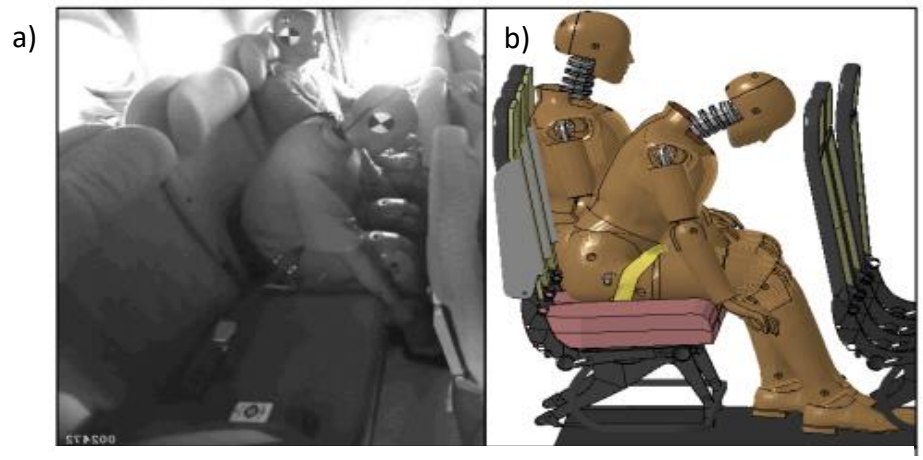

Figure 1 Test environment a) physical test b) FE simulation

While this test was insightful, it used ATDs to represent the human body (50th male: Hybrid II, Hybrid III FAA, 5th female: Hybrid III, 95th male: Hybrid III), as they are widely utilized for impact test research under various loadings. For example, under high-rate vertical loading, such as military vehicle underbody blast (UBB), a stiffer response of the Hybrid-III pelvic structure was reported as the corresponding PMHS response[13]. Additionally, no significant differences were observed in the peak T1 vertical acceleration of Hybrid III vs. PMHS at the T1 level. Still, peak vertical acceleration in the PMHS head was significantly lower than in Hybrid III due to the stiffness of the Hybrid-III neck [13]. Similarly, higher ATD stiffness was considered the leading cause of differences in ATD injury predictions relative to PMHS [25]. While PMHS physical testing would allow for the most comprehensive investigation of the F28 aircraft, they are costly and challenging to work with. A middle ground between PMHSs and ATDs is FE models of the human body, which have been validated based on PMHS tests [16-18]. Biofidelic

FE human body models (HBMs) have recently been developed to predict occupant response to complex loading environments. Two of these widely used models include the Global Human Body Models Consortium (GHBMC) [16] and the Total Human Model for Safety (THUMS)[19]. These models have been extensively validated in various automotive loading scenarios [16, 19] and used to predict human injury risk during impact; however, their capability to predict injury within realistic full-scale aircraft crash environments has not been extensively studied. The GHBMC has, however, been utilized to evaluate injury response in rotary-wing aircraft impacts [18] and underbody blast loading[26]. The THUMS has been used in vertical loading scenarios evaluating underbody blast implications [27]. In addition, studies have utilized the FE simulation tool LS-Dyna to simulate aircraft crash situations for over 20 years[10]. While these studies have evaluated and proven THUMS and GHBMC as valuable tools for injury research, limited data that compares the two HBMs in realistic full-scale aircraft crash environments is available.

Thus, this study aimed to simulate the GHBMC and THUMS HBMs in the previously developed Fokker F28 full-scale crash FE setup to explore the utility of these models for injury prediction in aircraft environments [24]. The GHBMC and THUMS responses were compared in terms of the magnitude and mechanism of injury. In addition, this is the first study to compare GHBMC and THUMS models in an aviation setting directly and may determine the advantages and disadvantages of these models for these loading conditions.

Methods:

Validation of F28 Impact Setup Model:

A previous numerical study developed the models of breakout seats and airplane interiors utilized for this study [24]. This model contains two rows of seats, the seat row containing the surrogate occupant and the forward seats, to account for the interactions between the model and the forward seatbacks. The seats were developed using manufacturer-provided CAD geometries and component testing to characterize material models for the included seat components [28]. The physical test utilized an assortment of eight different ATDs, including Hybrid II, Hybrid III FAA, and THOR 50th percentile dummies. The other dummies included alternate-sized dummies and a WIAMan dummy that was not computationally recreated and analyzed in this study. The validation simulations were performed utilizing the FAA Hybrid III 50th version 1.2.3 FEM [29] and the THOR version 2.1 [30, 31]. The validation of the seat environment model utilizing the FAA Hybrid III model represented both the Hybrid II and FAA Hybrid III dummies used in the physical testing due to the model availability limitations. While this utilization validates both physical dummies' lumbar load response[12, 32], it is not considered a valid representation of the head-neck responses from the physical tests [12, 32]. This is due to differences in the construction of the neck components between the two Hybrid dummies. Therefore, the Hybrid II neck and head test responses and neck/head injury predictions were not compared with the corresponding simulation data. Other test vs FE results were compared utilizing ISO 16250, an international

objective rating standard for validating FE models [33, 34]. ISO 16250 specifies a method for calculating the level of correlation between physically tested time-history signals and simulated signals. While this validation approach has some limitations related to the available ATD models mentioned above, the reasonable results obtained suggest that the setup model reasonably replicates the F28 impact environment. Therefore, human models could be simulated realistically to approximate airplane impact conditions.

Crash Conditions:

This study recreated eight out of the twenty-four crash conditions evaluated in the full-scale F28 crash in free fall boundary conditions, with the aircraft impacting the soil bed with 19.9 m/s horizontal and 9.7 m/s vertical velocities (Figure 2). These eight conditions correspond to 50th-percentile ATDs for comparisons to the 50th-percentile HBMs implemented in this study. The sixteen other crash conditions were excluded due to incomplete test data and/or physical dummies that did not have representative FE models for validations and comparisons. These conditions are labeled and referenced by their row number and seat-lettered label. In addition, these eight conditions span the aircraft's main body from row 3 through row 10.

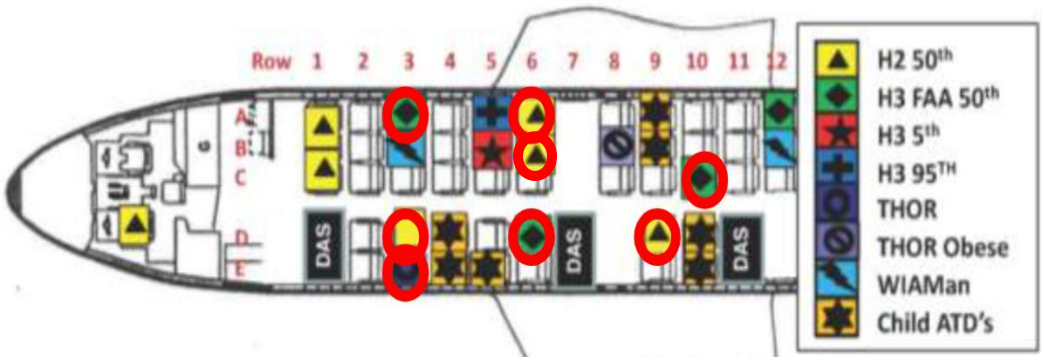

Figure 2 Crash conditions evaluated in this study. This figure is modified from a previous study [23].

All conditions in this study were recreated computationally and validated against the physical test utilizing ATD model comparisons. The eight crash conditions (pulses) implemented for each HBM were distributed among four-seat configurations, representing seat layouts used within the aircraft (Figure 3). These crash pulses were all 250ms long and applied accelerations in vertical and longitudinal directions relative to the aircraft. The 3-seat model was utilized to simulate both the port and starboard side seats, as the A/B and D/E seat geometries were symmetric. The test conditions in this study are labeled as row ("R") followed by the row number and then the seat letter associated. The Conditions R3A, R3D, R6A, and R6D were all simulated in the seat A model setup (Figure 3a). Condition R9D utilized seat A with the removal of the forward seat (Figure 3b). Conditions R3E and R6B utilized seat B (Figure 3c). Finally, condition R10C utilized the seat C configuration (Figure 3d).

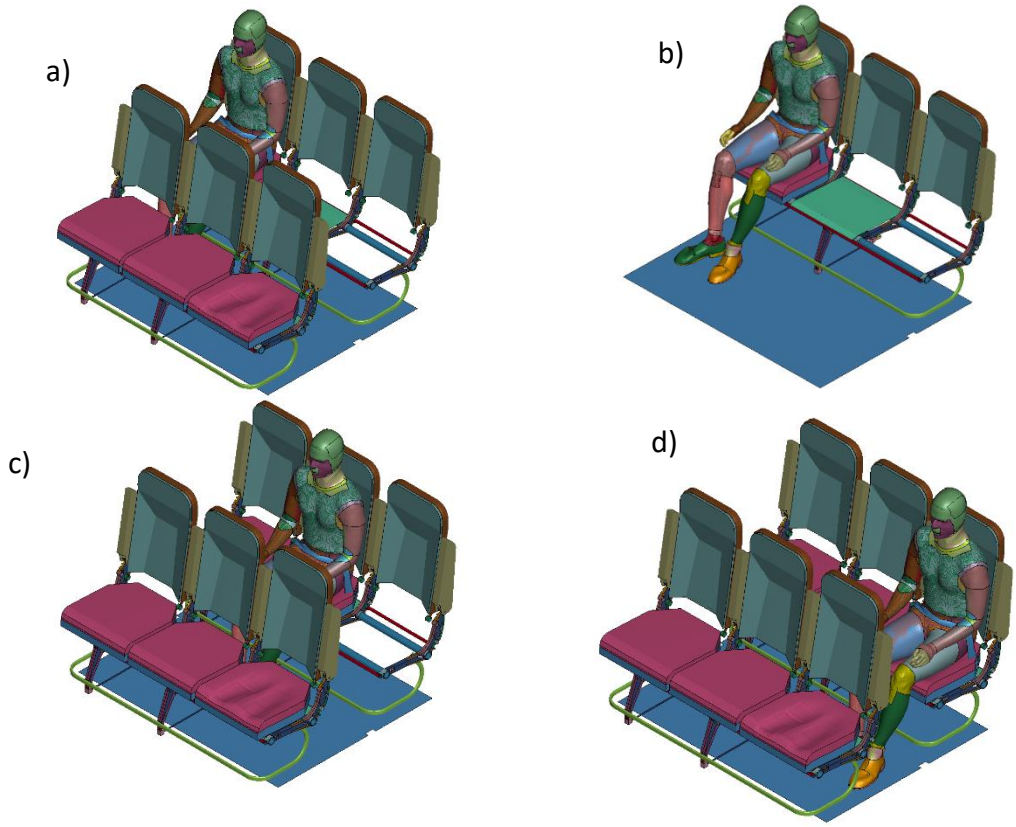

Figure 3 Seat conditions for all tests a) Seat A/D, b) Seat D without forward seat c) Seat B/E d) Seat C

The crash pulses implemented for this study originated from the accelerometers placed underneath the seats during the full-scale crash test [24]. These accelerometers measured the X and Z directional accelerations at the floor level of each row and were implemented into the respective seat environments. Adjacent seats were modeled to share the same pulse. The corresponding pulse and seat positions yielded the eight test conditions in this study (Table 1). These six pulses (Appendix A) were implemented as prescribed accelerations to the floor of each seat model.

*Table 1 Test, seat, and pulse associations (shared pulses are shaded). *Condition R9D had the forward seats removed from seat A/D to represent the physical F28 configuration.*

Test condition	Seat Model	Pulse
R3A	A	3A
R6A		6AB
R3D		3DE
R6D		6D
R9D	A*	9D
R6B	B	6AB
R3E		3DE
R10C	C	10C

HBM Implementation:

The GHBMC male 50th percentile occupant detailed model (v6.0 [35]) and THUMS male 50th percentile occupant model (v6.1 [19,36]) were selected to be used in the FE crash simulations. The seat model and crash pulse were converted to the respective unit systems for THUMS (mm, ton, sec) and GHBMC (mm, kg, msec). Two HBM postures were examined: upright (Figure 4a) and braced (Figure 4b). In the upright posture, the HBMs were oriented neutrally upright, the HBMs' hands rested on the legs, and the feet contacted the floor. In the braced posture, the HBM leaned forward with their arms braced against the front seat. No muscle activation was modeled in this study.

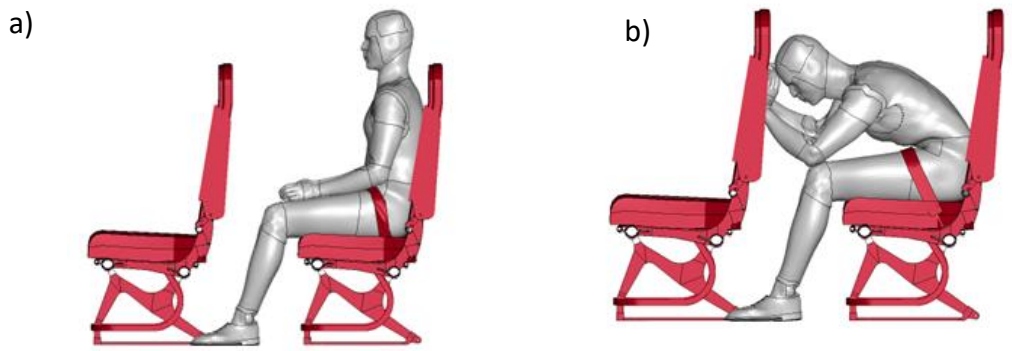

Figure 4 HBM postures a) upright b) braced

Marionette positioning, a technique that involves simulating with contracting beam elements "pulleys," was used to position the GHBMC model into the required upright position. The GHBMC model was then implemented as the reference position to achieve similar spinal, foot, and head positions with the THUMS marionette simulations. The final relative upright positions are shown in an overlay (Figure 5). Next, gravity was applied in a 150-ms simulation to settle each HBM into the seat and create the appropriate seat deformation. The lap belt was placed on the HBMs for all test conditions using the seat belt fitting tool. [37]. To preserve the initial conditions of seat deformation, the deformed top seat cushion was translated and re-constrained to represent each seat test location.

Figure 5 Overlay of final upright positioning
Green: GHBMC
White: THUMS

A braced positioning was implemented and evaluated for the R6B test condition to represent the dummy position utilized in the physical test. To place both HBMs in the braced position, both models were first settled in the upright condition in the Seat B configuration. Marionette pulleys were placed on each model's head, arms, and hands. The THUMS documentation admits that substantial alterations in the posture of the THUMS model are likely to cause errors in the muscle-tendon complex models [36]. As recommended in the THUMS documentation, to avoid these instabilities, the model braced positioning and crash pulse were run in the same simulation [36]. The same approach was applied to the GHBMC to maintain consistency between the models. The marionette pulleys were implemented for 150ms before the crash pulse. After this 150ms precrash positioning, the resulting position resulted in the HBMs being in similar braced positions for the 6B test. However, due to differences in compliance of the various extremities to the same marionette pulleys, there is more variation in the initial position between the two braced positions than the upright position (Figure 6).

Figure 6 Overlay of final braced positioning
Green: GHBMC
White: THUMS

Injury Metric Calculation:

Injury risk probabilities were calculated based on each simulation's maximum head and neck injury metric value. The injury risk metric calculated in this study included the head injury criteria (HIC15) and neck injury criteria (N_{ij}) metrics. HIC_{15} is the standard head injury criterion for motor vehicle safety calculated utilizing the head acceleration at its center of gravity [38]. Calculations for HIC_{15} are performed as the integral of acceleration over a 15ms time interval:

Equation 1:

$$\mathrm{HIC}_{15} = 15\left(\frac{1}{15}\int_{t1}^{t2} a(t)dt\right)^{2.5}$$

N_{ij} is used to characterize injury risk within the cervical spine. The injury metric was developed using piglet test data scaled to human anthropometry [38]. The calculations utilize critical intercepts to normalize force and moments measured between the first and second neck vertebrae and then linearly sum the two measures as:

Equation 2:

$$N_{ij} = \frac{F_z}{F_{int}} + \frac{M_y}{M_{int}}$$

The head and neck metrics were converted to a probability of Abbreviated Injury Scale (AIS) 3+ injury (Table 2). AIS is a scale utilized to measure the threat to life associated with an injury. A score of 3+ denotes an injury that is serious or worse. AIS is an anatomically-based coding system that classifies the severity of injuries based on body region [39]. The scale spans from 1 (minor) to 6 (fatal). Researchers chose AIS 3+ for this study with the ideology that moderate (AIS 1) and minor (AIS 2) injuries may be less preventable in aerospace crash situations. Therefore, researchers should prioritize serious or worse injuries for research and, in turn, improve safety features. Lumbar vertebral loading was quantified using peak axial force, which allowed for direct comparison to the previously conducted ATD testing.

Table 2 Injury Metrics and Injury Risk Probability Functions

Body Part	Injury metric	Injury Risk Probability Function
Head	HIC_{15}	$P(AIS\ 3+) = \emptyset\left(\frac{ln(HIC_{15}) - 7.45231}{0.73998}\right)$ [38]
Neck	N_{ij}	$P(AIS\ 3+) = \frac{1}{1+e^{(3.227 - 1.969 * N_{ij})}}$ [38]

The GHBMC model included sufficient digital instrumentation to compute the head, neck, and lumbar injury metrics used in this study. Digital instrumentation in FE models refers to specific elements or sections of elements denoted as load cells or accelerometers where the time-history of forces or accelerations is output for analysis. The THUMS model digital

instrumentation was limited to node output data for various markers in the body. To implement the neck injury metrics and measure spinal loading force in the THUMS model, force cross-section outputs were created at the C1-C2 (neck) and L5 (spine) vertebra to match the virtual instrumentation included in the GHBMC model. To calculate N_{ij}, the cross-section at the C7 vertebra included the deformable tissues along this vertebral plane. The GHBMC and THUMS models included representative Head center of gravity (CG) nodes. The head CG node is a digital representation of an accelerometer positioned roughly at the head's center of gravity, which is used to analyze head injuries. The construction of the THUMS used a node in the model's temporal lobe representation, whereas the GHBMC model constrained the head CG node to the stiffer skull material. Preliminary simulations identified unrealistically high magnitude accelerations in the THUMS head CG node due to brain deformations. These deformations were caused by compression of the brainstem, cerebellum, and temporal lobe, which is caused by high vertical loading transferring through the spine into the brain. The head injury risk probability utilizing the original THUMS CG node reported a 100% probability of injury in every test, with resultant acceleration values reporting over 1000gs. Therefore, to create consistency between the HBMs, the head CG node for the THUMS model was constrained to the rigid skull, as in the GHBMC model.

Model Modifications and Model Stability:

Both models required modifications to ensure stability through the entire 250 ms crash pulse. During the GHBMC runs, the simulation failed during the impact of the face on the forward seat back. This necessitated the addition of strain-based element erosion for the

affected parts in the face flesh and the face bones. The THUMS model, in turn, required strain-based element erosion added to a ligament in the left shoulder. These modifications allow for deleting problematic elements above a threshold strain value. These modifications are believed to affect the recorded injury metrics insignificantly; however, they were necessary to stabilize the models during the impact simulations.

Results and Discussion:

Seat Model Validation:

The seat model, which included the seat, belt, and contact definitions between the occupant model and seat components was validated through a direct simulation comparison between tested ATDs and representative ATD models [24]. The ISO/TR-16250 curve rating methodology was used to quantitatively assess the correlation between simulation and test for this validation. This standardized curve comparison methodology scores the correlation between two curves on a scale between 0 (no correlation) and 1 (exact match). Correlation is calculated as a function of phase, shape, and peak value between the two compared curves. In this analysis, a score of 0.5 or greater was considered an adequate prediction of ATD response. The 0.5 threshold used in this analysis was previously defined based on a blind comparison between qualitative assessment of breakout occupant FEM correlation adequacy made by subject matter experts in aerospace crashworthiness and computed ISO/TR-16250 scores. Example plots showing scores above and below this threshold are shown (Figure 7). In a comparison of lumbar force time history (Figure 7a), the model predicts peak force but it does

not fully capture the loading shape and phasing of the unloading response (0.56 score). Although there is likely room for improvement this response would be considered acceptable for validation of the model for this study's primary purpose of comparing the two HBMs. The R6B pelvis acceleration in the Z direction received a correlation score of 0.39 (Figure 7b). This low score was caused by the model poorly predicting the shape and peak value of the response. Response phasing was partially in line with the test but significant improvement would be required to consider this response validated.

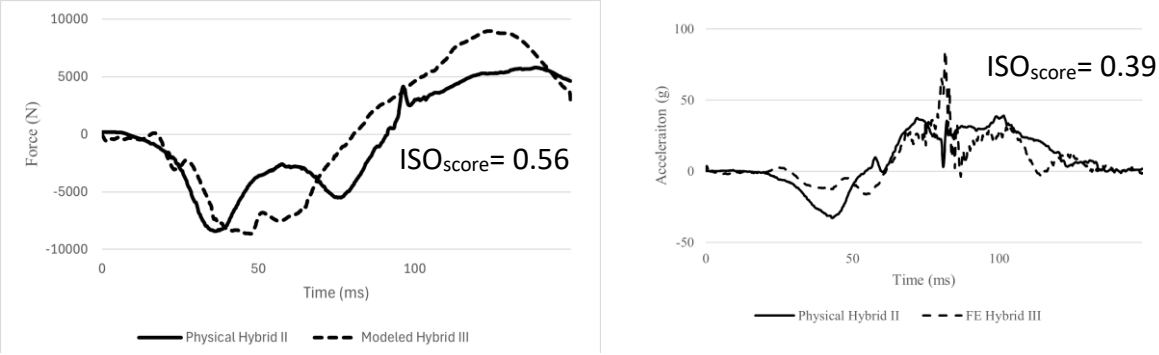

Figure 7 Examples of FE vs test data correlation a) Hybrid II/III Lumbar for test R9D b) Hybrid III Pelvis Z acceleration for test R6B

The ISO/TR-16250 scores for each response evaluated in the seat model validation process were reported (Table 3). The closest predicted responses were Z (vertical) direction acceleration and force metrics. The lumbar loads for the Hybrid III FE model closely matched the phasing response and lumbar load of all tests which suggest a reasonable validation of the seat setup model. However, the peak lumbar axial force of Hybrid III FE model was slightly overpredicted for tests R3A, R3D and slightly underpredicted in tests R6D and R9D. The ISO correlation score of the pelvis fell above the 0.5 threshold for all Z direction outputs except for the Hybrid II pelvis in tests R6B and R9D. The correlation scores for the X (horizontal) direction

had most of the responses falling below the correlation threshold of 0.5. The Hybrid II correlations are the most variable due to the nature of their representation by the Hybrid III model. However, in the spine, due to its similar construction between Hybrid II and Hybrid III, there is still a close correlation.

Table 3 FEM Simulation ISO Correlation Scores

Seat	Head AX	Head AZ	Chest AX	Chest AZ	Pelvis AX	Pelvis AZ	Spine FZ	Neck FX	Neck FZ	Neck MY
FAA Hybrid III										
R3A	0.57	0.53	NA	0.84	0.34	0.60	0.79	0.47	0.55	0.50
R6D	0.42	0.64	0.55	0.67	N/A	N/A	0.69	0.40	0.66	0.41
R10C	0.28	0.54	0.29	0.75	N/A	N/A	0.57	0.19	0.52	0.49
Hybrid II										
R3D	0.44	0.63	0.48	0.77	0.37	0.70	0.74	N/A	N/A	N/A
R6A	0.33	0.61	0.41	0.82	0.27	0.66	0.78	N/A	N/A	N/A
R6B*	0.30	0.59	0.62	0.56	0.26	0.39	0.59	N/A	N/A	N/A
R9D	0.43	0.63	0.27	0.67	0.40	0.41	0.56	N/A	N/A	N/A
THOR										
R3E	0.69	0.58	N/A	N/A	0.24	0.73	0.51	0.48	0.48	0.35

Signals with scores above 0.5 are shaded.
*Braced position.

Correlation scores in the X (horizontal) direction were lower than those in the Z (vertical) direction. The low correlation scores in the X direction may be linked to several factors in model development. First, the vehicle model was ineffective in predicting the horizontal acceleration response of the structure in the impact scenario, which reduced the fidelity of

horizontal loading in the occupant models. Second, the X response was more sensitive to variability in the test setup, such as ATD positioning, making it more difficult to predict precisely. Thus, due to the limited correlation achieved by the ATD models in the X direction, only the Z direction results were considered valid for comparison to the HBMs in this study. The principal injury metric compared between ATD and HBMs was peak lumbar spine compressive force.

Overall Injury Metrics:

The average injury risks of the HBMs across all the impact conditions are reported in Table 4. The GHBMC model predicted higher injury risk probabilities in the head and neck regions than the THUMS model. The same trend was observed for the maximum axial lumbar spine force. However, both average HBM maximum lumbar force values were lower than the corresponding ATD average (8.0 kN).

Table 4 Average injury risk values

Body Component	GHBMC	THUMS
Head	29.89%	17.19%
Neck	21.15%	5.34%
Lumbar Force	4.8kN	3.3kN

Head Injury Results:

The GHBMC and THUMS head injury risks varied depending on the test case (Figure 8). In all test conditions except R6B, the THUMS model reported lower head injury risk than the

GHBMC model. Test condition R3E resulted in the lowest discrepancy between the models, and the test R9D condition resulted in the highest discrepancy between the model responses.

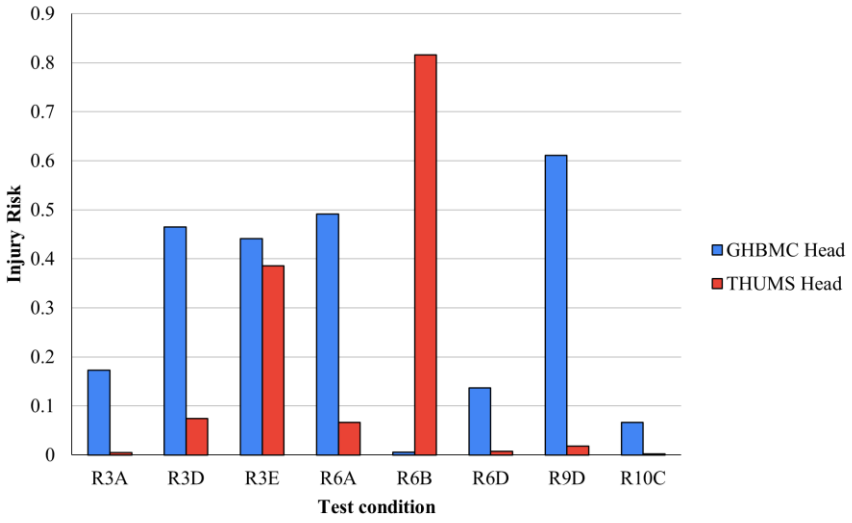

Figure 8 Head injury risk probabilities for all test conditions.

Test condition R6B resulted in a substantially more significant head injury risk reported by the THUMS model. Both models exhibited similar kinematics through the majority of the simulation. At 100ms, however, the THUMS model had a high peak in acceleration resulting from a head impact on the lower rear bar of the forward seat. The GHBMC model did not report this high acceleration because it remained in contact with the forward seat back (Figure 9).

a) 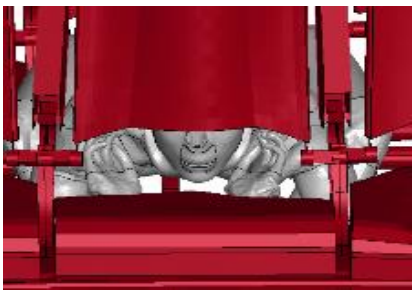

b) 

Figure 9 The kinematics at head at 100ms. a): GHBMC b): THUMS (Test R6B)

Outside of the R6B condition, the GHBMC model predicted higher head injury risk in all of the remaining test conditions than THUMS. The most significant discrepancy was recorded in the test R9D condition, with a difference of 59%. In test R9D, the peak acceleration of the head CG for the GHBMC model was approximately double the peak of the THUMS model (Figure 10).

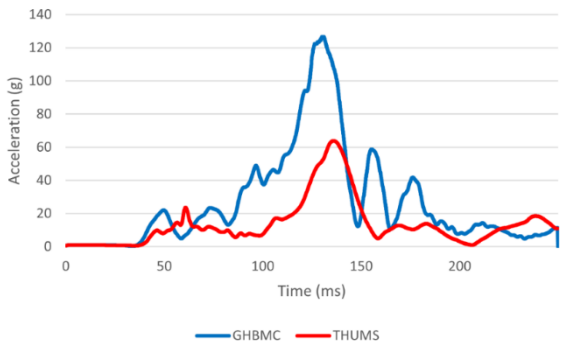

Figure 10 Time histories of the resultant acceleration of GHBMC and THUMS CG nodes (Test R9D)

In the R9D test condition, the kinematic response of the models was not substantially different. The GHBMC model lost contact with all floor elements around 125 ms when the head injury occurred. On the other hand, the THUMS model remained in contact with the floor (Figure 11). In all different ways, the kinematics remained similar to each other. The differences in floor contact are not expected to affect the head cg's accelerations significantly. However, the large discrepancy in the injury metric measured by each model is likely a sign that the GHBMC may be more sensitive to the inertial acceleration of the head. Due to differences in HBM construction and weight distribution, the GHBMC model distributes higher loads and accelerations through the head. In contrast, the THUMS model may distribute these same forces more successfully through the legs and seatbelt. The substantially differing response in head injury risk in a non-head impact test condition shown in R9D is an important area for

future evaluation. Further developments in occupant restraints may be necessary if there is a higher risk of head injuries for passengers without forward seatbacks.

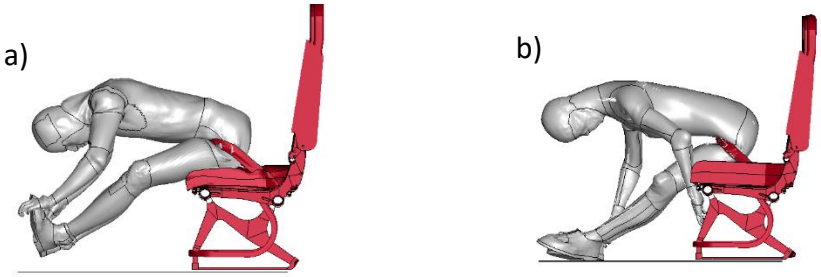

Figure 11 The kinematics at the moment (125ms) of peak HIC during the simulated crash pulse. a: GHBMC b: THUMS (Test R9D)

Neck Injury Results:

Neck injury for THUMS showed a lower injury risk than GHBMC for all crash pulses (Figure 12). Both models show similar trends, with the highest injury risk reported in test R9D and the lowest in test R6B. The highest injury risk discrepancy can be seen in test R9D, which can be attributed to the differences discussed for head injury during this test condition (Figure 10).

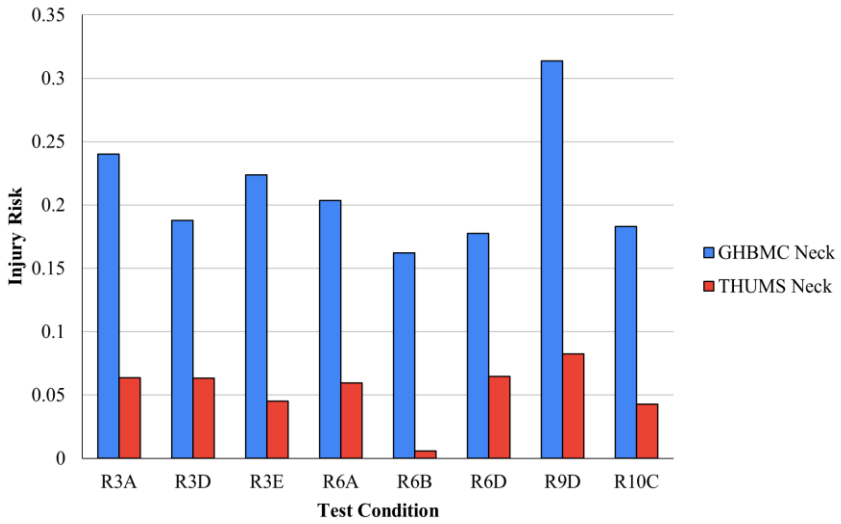

Figure 12 Neck injury risk for all test conditions.

Kinematically, there is a substantial difference between the neck response of these models, creating the differentiation between neck forces predicted by each model. The upper region of the THUMS was found to be more compliant than the GHBMC, as demonstrated by the "s" shaped compression of the GHBMC neck in the test R3A condition (Figure 13). Greater neck flexibility may have blunted the forces transferred into the upper neck of THUMS. This high flexibility and blunting of troops through the skull and back contact are apparent factors in the reported neck injury metrics in all test conditions. These differences may also compound and influence the lower injury exhibited for the THUMS head in many test conditions.

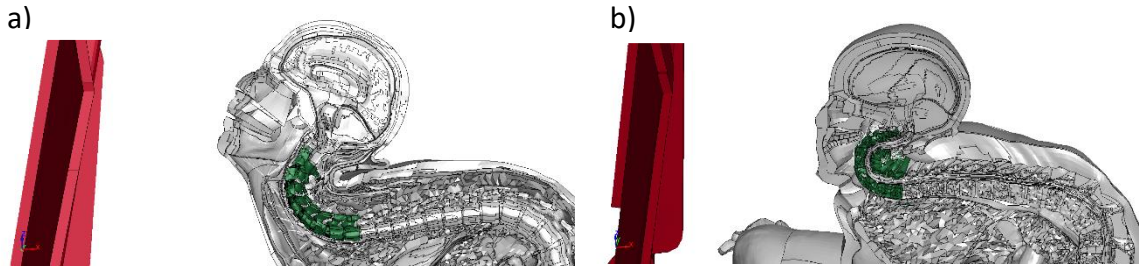

Figure 13 The neck kinematics. a) GHBMC b) THUMS (Test R3A)

Spine injury results:

The spinal loading was the most accurately validated dataset from the ATD modeling. Both HBMs varied in their comparisons to each other and the ATD tests. The GHBMC model generally predicted higher maximum values of spinal lumbar force than the THUMS model in the simulated test conditions (Figure 14). Test R6B was the only test in which the maximum lumbar force recorded in the GHBMC model was reported to be lower than in the THUMS model. The maximum axial spinal force was higher in the modeled ATD tests than that predicted in the HBM simulations for most test conditions evaluated (6 out of 8). The modeled ATDs produced lower spinal forces than the HBMs in test R3E and lower than the GHBMC in test R3A.

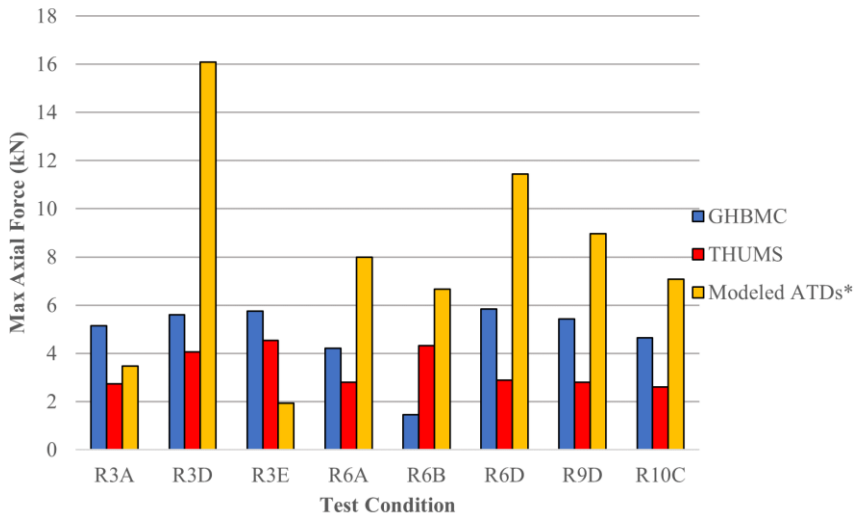

Figure 14 Maximum magnitude of lumbar axial force for all test conditions
**Modeled ATDs refer to Hybrid III (R3A, R3D, R6A, R6B, R6D, R9D and R10C) and THOR (R3E) FE model data*

The R6D simulation reported the most significant difference between the GHBMC and the THUMS, which reported lumbar axial forces. Kinematically, for this test, the HBMs did not produce substantial differences. Both models show similar spinal curvature at the time of maximum spinal loading (Figure 15).

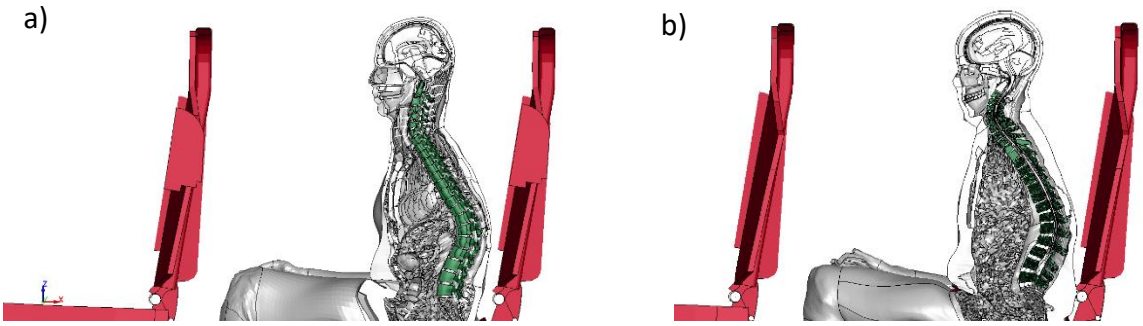

Figure 15 The spine kinematics at 47ms. a: GHBMC b: THUMS (Test R6D)

The similar spinal curvatures between the two HBMs and differing lumbar force values indicate that the construction of the models led to the differential distribution of forces into the abdomen for the same loading conditions. With the current virtual instrumentation of the HBMs, it was difficult to determine the precise mechanism of loading distribution through the abdomen, which resulted in the lumbar axial force discrepancy between the models. With neither model being directly developed nor validated for high vertical loading, this study cannot draw direct conclusions as to which model may be more accurately representative in this loading case.

Test condition R6B was the only case to show higher spinal loading for the THUMS model compared to the GHBMC. The GHBMC model exhibited a more horizontal spine than the THUMS model during the peak lumbar forces reported by both models (Figure 16). The

horizontal position in the GHBMC reduced the amount of vertical acceleration transferred to axial force loading on the spine. In addition, the highly compliant neck of the THUMS model allowed for compression and shoulder contact from the THUMS model to the forward seat back. This contact with the upper body of the THUMS model increased the amount of horizontally directed acceleration translated into the axial loading of the spine.

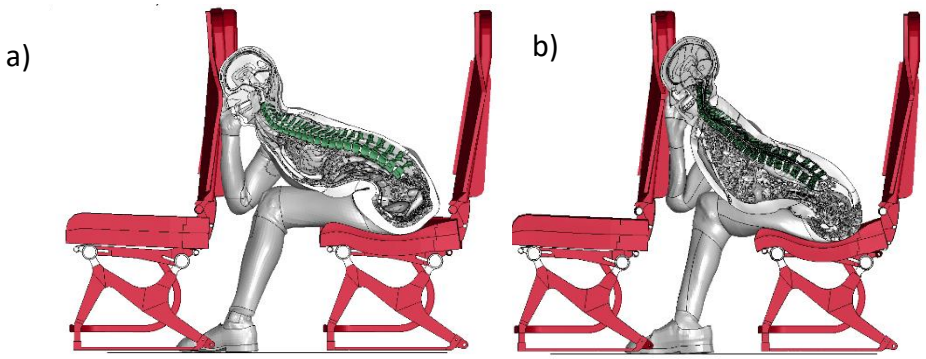

Figure 16 The spine kinematics at 45ms. a: GHBMC b: THUMS (Test R6B)

Higher spinal axial forces were expected to be reported by the ATD models (especially for Hybrid III). These ATD models utilize a more simplistic and rigid design for the spine and thoracic cavity than the HBMs(Figure 17). For example, the lumbar spine components of Hybrid III have a solid rubber structure with a curvature opposite the natural human shape and a steel box to represent the thoracic spine[40]. These more rigid structures allow limited distribution of forces away from the spine. In contrast, both HBMs diffuse vertical force into the abdominal cavity's compressible elements of muscle and fat.

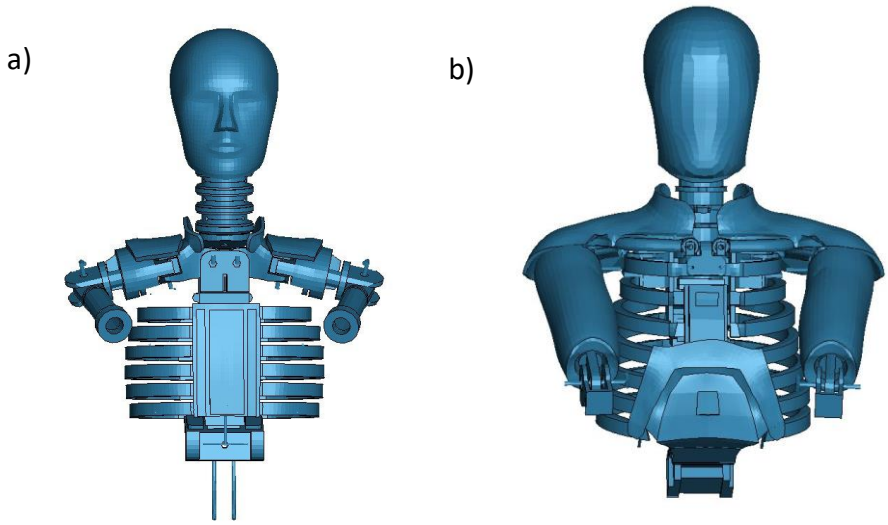

Figure 17 Thorax construction of Hybrid III and THOR ATDs. a: Hybrid III b: THOR

Overall Model Comparisons:

The GHBMC model predicted higher risk for every metric reported than the THUMS model except for the head injury and spinal force in test R6B. Each model in this study is treated as a valid surrogate for a human body. Therefore, in each case, the highest injury risk values reported are treated as a possible realistic mechanism of injury. The consistently highest results reported by the GHBMC model are helpful in further understanding possible mechanisms of injury that may occur to a human body under these loading conditions. By evaluating the reported mechanisms of injury and implementing safety features, reducing the injury risk reported for all models tested may be possible. In most tests, the HBMs yielded vastly different reported injury metrics. The main kinematic difference appeared in the neck of the THUMS model, which seems to be more flexible than the GHBMC model. In addition, the GHBMC generally produced higher injury metric values. These results suggest that the GHBMC

may provide a more conservative injury risk assessment than the THUMS, which aligns more with current ATD predictions. The more conservative predictions may be more beneficial because they have less likelihood of leading researchers to overlook dangerous injury mechanisms.

In 2 out of 8 cases, the GHBMC reported higher spinal loading forces than the ATD models. This shows that the ATD models produce more conservative injury risk assessments than the HBMs. The two cases of higher injury risks reported by the GHBMC illustrate a potential gap within the predictiveness of the ATD models. These "gaps" are conditions where ATD models could report low or no injury risk. Therefore, without using HBMs, researchers may not identify some situations where human occupants are at risk for injury.

The effect of the braced positioning on occupant injury risk also differed between the HBMs and the ATD models. Both the ATD and GHBMC suggested a reduction in predicted injury metrics through the use of this position when compared to the unbraced R6A. However, the THUMS model reported higher injury risk through this positioning. The braced position is a potential safety technique in emergency landings to reduce injury risk. Disagreements between the various models illustrate a possible need for further evaluation to confirm the benefits of bracing.

This study identified variability in aerospace loading responses from each model utilized. For many test conditions, the kinematic response was the driving difference between discrepancies between the HBMs. However, in some cases, such as the R9D head injury comparison, it was apparent that inherent model differences contributed to variation in the

reported metrics. The GHBMC model appeared to be sensitive to nonimpact head injuries. The THUMS model exhibited a highly compliant neck and reported increased injury risks through braced positioning. ATD lumbar loads surpassed most of the results reported by the HBMs in these tests. However, there are cases where the HBMs reported high injury risk that may not be identified solely through ATD evaluation. Without extensive PMHS testing, it is irresponsible to conclude the complete accuracy of any method to encapsulate the injury risk within an airplane crash-loading scenario. The HBMs were extensively validated at the component level against PMHS data for various injury mechanisms observed in occupants and pedestrians[41-46] during traffic accidents before accepted utilization in complete accident validations. Therefore, a similar process could be followed to increase the confidence in HBMS predictions in the simulation of airplane accidents. For example, new PMHS tests for HBMs validation for airplane crash loadings may be designed utilizing the HBM and ATD results presented in this study.

Study Limitations and Future Work:

This study was limited in its sample sizes of seat conditions. With only eight crash pulses examined within four seat conditions, there is not enough data to calculate the simulation results' statistical significance. In addition, limited PMHS validation is available for these HBMs in the high vertical loading environments of aerospace crash scenarios.

Current developments in human body modeling include the design of more advanced HBMs for the specific use case of aerospace investigations [47]. Further insight may be gathered from future exploration into the variability in human seating positioning, which HBM models may be

able to represent better than ATDs. A direct comparison to ATD injury response was limited by test instrumentation and model validation in the horizontal direction. Future work focused on the head and neck response of the HBM and ATD models in the aerospace crash-loading environment is recommended to characterize better the effect of the kinematic differences identified.

Conclusion:

The study identified differences in HBMs and ATD loading responses, resulting in differences in injury risk prediction based on seating and positioning effects within a full-scale aircraft crash test environment. These results demonstrate the value of utilizing advanced HBMs to assess aerospace crash environments to characterize potential injury risk mechanisms and sensitivities fully.

This study identified the potential for HBMs and ATDs to show differing trends and responses to the same testing conditions. Identifying these discrepancies is essential in developing and evaluating safety features in the aerospace environment. HBMs are valuable tools that allow researchers to identify mechanisms of injury not captured by ATDs, and their use may provide beneficial information for improving safety technologies. However, the complexity of these HBMs requires substantial computational power. Therefore, due to the benefits of both model types, it is essential to use a combination of tools for further research in aircraft safety.

Among the HBMs, both models have benefits and drawbacks when used in high-loading environments of aircraft modeling simulations. The GHBMC has value in its included virtual

instrumentation, and injury metric responses are more in line with those recorded by the ATDs. However, the THUMS model provides the benefit of higher accessibility and free access. In addition, the THUMS model showed similar kinematics to the GHBMC in most of the test conditions evaluated in this study. The main difference in model kinematics occurred with the apparent higher flexibility of the THUMS neck. This resulted in higher bending and lower injury response than the GHBMC for all eight test conditions. The GHBMC injury risk surpassed the THUMS-reported injury risk for 22 out of 24 metrics studied, thus providing a conservative safety assessment.

Both models require further validation to be better utilized as predictive tools for the high vertical loading environments of aircraft crash testing. However, current studies using the implementation of safety features may still find benefits from including one or both HBMs. The computational tools utilized in this study are expected to continue to develop, allowing for a faster and more informative way to test aircraft safety than traditional physical testing, as they are currently being utilized for car crash safety studies. Future research is planned to continue using these models in aircraft loading environments and explore alternative models that include more diverse sizing and positioning variations to support the overall goal of increasing aircraft safety for all occupants.

Chapter 3: Study of Advanced Occupant Models to Quantify Injury Risk for eVTOL Vehicles

Introduction:

The development of electric Vertical Take-off and Landing (eVTOL) vehicles creates an opportunity for revolution in the world of urban air travel. These vehicles are designed to provide sky-based transportation within urban environments while also allowing for efficient transport for cargo, people, and emergency services. eVTOLs are designed to be small and lightweight for mobility and efficiency. In addition, many of these vehicles combine vertical takeoff capability with the ability to transition to more standard fixed-wing aircraft flight. These unique features create new loading conditions in emergency landing situations that may necessitate novel safety features for passengers.

Recently, the Federal Aviation Administration (FAA) added powered lift to the definitions in § 110.2 of title 14 of the Code of Federal Regulations [47]. This added definition begins the regulation process that applies to eVTOLs. However, this update focuses on operation and utilization of these vehicles rather than safety in the design process. The safety regulations of standard aircraft may apply to the novel design of the emerging eVTOL market. However, more research into potential mechanisms of injury in unique vertical loading environments may be required.

Researchers at the National Aeronautics and Space Administration (NASA) Langley Research Center (LaRC) have looked extensively at developing tools for eVTOL testing and safety quantification. A main avenue of research in these novel eVTOL aircrafts is safety

considerations in seat design. Researchers at NASA LaRC have performed extensive seat testing utilizing an anthropomorphic testing device (ATD), the Hybrid III FAA, in a 30-foot drop tower to compare a variety of potential seat designs and materials for implementation in these vehicles [48]. ATDs are valuable tools for understanding mechanisms of injury that occur in emergency landing situations. However, the Hybrid III, developed over 40 years ago by General Motors [11] for automotive safety, has different usage. The Hybrid III was originally designed to represent human response to impact scenarios corresponding to automotive frontal impacts with limited datasets for alternate loading scenarios. Methods for using these physical devices in aircraft impact testing have been improved with modified models such as the Hybrid III FAA model, but due to their rigid construction for repeated testing they are limited in their biofidelity. Other developments include a host of newer and more biofidelic ATDs such as the Test Device for Human Occupant Restraint (THOR) [49, 11]. However, some limitations associated with ATDs perpetuate. One such limitation is the limited variability of positioning possible with these rigid ATDs. These limitations are particularly relevant in aerospace crashworthiness as alternate positioning (e.g. bracing) has been utilized as a safety tool for airplane crashes for over 20 years. Studies as early as 1993 by Brownson [50] biomechanically evaluated the braced positioning. Novel aircraft development requires evaluation of similar techniques to develop safety procedures for these vehicles.

While Postmortem Human Surrogates (PMHS) (cadavers) are inherently biofidelic, it is challenging to work with PMHS and tests are costly. More efficient and cost-effective alternatives to physical testing are finite element (FE) models of the human body which have

been validated to PMHS tests. Recently, newer and more biofidelic FE human body models (HBM) have been developed for crash safety analysis applications [19,51]. One of these widely used models includes the Global Human Body Models Consortium (GHBMC). This model has been extensively validated in various occupant [52] and pedestrian [41] loading scenarios and used to predict human injury risks during impacts. The selection of the GHBMC was influenced by its previous usage in a study of airplane crash scenarios. The study showed the GHBMC to be computationally stable with sufficient instrumentation for aerospace injury risk assessments and reasonable computational cost [53]. Furthermore, tools such as ANSA BETA (Beta CAE Systems, Farmington Hills, MI, USA) allow for computationally inexpensive exploration of alternate positionings of the GHBMC [54].

There are limited data exploring the effect of posture on injury risk in vertical loading environments. Studies have utilized FE simulations to evaluate the effect of posture on pelvic fracture risk in underbody blasts which are similar in the vertical loading orientation to aerospace crash environments [55]. However, these studies utilize different loading magnitudes and frequencies as well as analysis metrics which may not be applicable to aerospace loading environments.

Researchers at NASA LaRC developed FE models which were representative of the vertical seat drop tests they performed. These models used seat geometries, and the various crash pulses which were implemented in the physical testing. To validate the loading conditions and seat materials to represent the physical tests, the response of the Hybrid III FAA FE model was compared with corresponding test data. Then, alternative occupant surrogate models, such as the GHBMC and THOR FE models, were simulated in these conditions to further understand

potential injury mechanisms within the studied impact environment. In addition, the GHBMC was used to evaluate the effect of positioning via lumbar flexion/extension on occupant injury risk.

Methods:

Model Environment:

This study used three seat models representative of the seat configurations investigated in the physical testing. The first was a generic aluminum bucket seat which will be referred to as "the rigid seat" (Figure 18a). This seat was modeled as a rigid aluminum material structure rigidly connected to the floor. The second seat model, "the energy absorbing (EA) seat", was the same generic aluminum seat with the addition of NASA designed EA tubes connecting the seat to the floor (Figure 18b). The final seat was a generic composite seat referred to as "the composite seat" (Figure 18c). The physical EA and standard setups (figure 18d-e) were utilized as references for the model development. In addition to the material differences, the composite seat had a slightly different geometry compared to the aluminum bucket seats. As with the rigid seat, the composite seat was rigidly constrained to the floor for these tests.

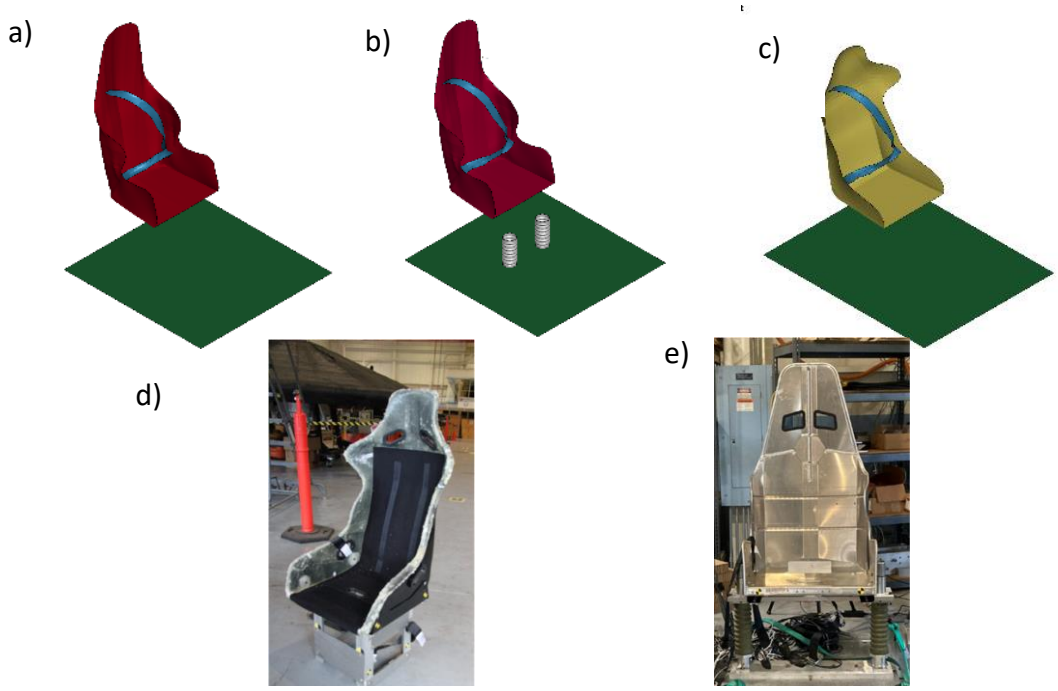

Figure 18 Seat models a) Rigid seat b) EA seat c) Composite seat

Physical seats d) Rigid seat e) Composite seat on EA setup

There were four crash pulses implemented in the physical tests to approximate potential vertical loading environments during an emergency crash of an eVTOL vehicle. These pulses (10 g, 19 g, 30 g, and 42 g crash pulse) correspond to approximations of emergency landing conditions defined by the Federal Aviation Administration (FAA) (14 CFR 23.562 and 27.562), and physical tests of a lightweight helicopter and a composite aircraft body dropped by researchers at NASA LaRC [56-59]. In the physical 30-foot drop tower test, these pulses were generated utilizing cardboard honeycomb stacks. Each of the four pulses were tested with the rigid seat. The EA and composite seats were only tested in the 19g and 30g pulses due to limited test data. During each physical test, floor level accelerometer data were extracted and

filtered to SAE CFC 60 for implementation in the simulation study. This resulted in eight unique crash pulses paired to each seat (Figure 19).

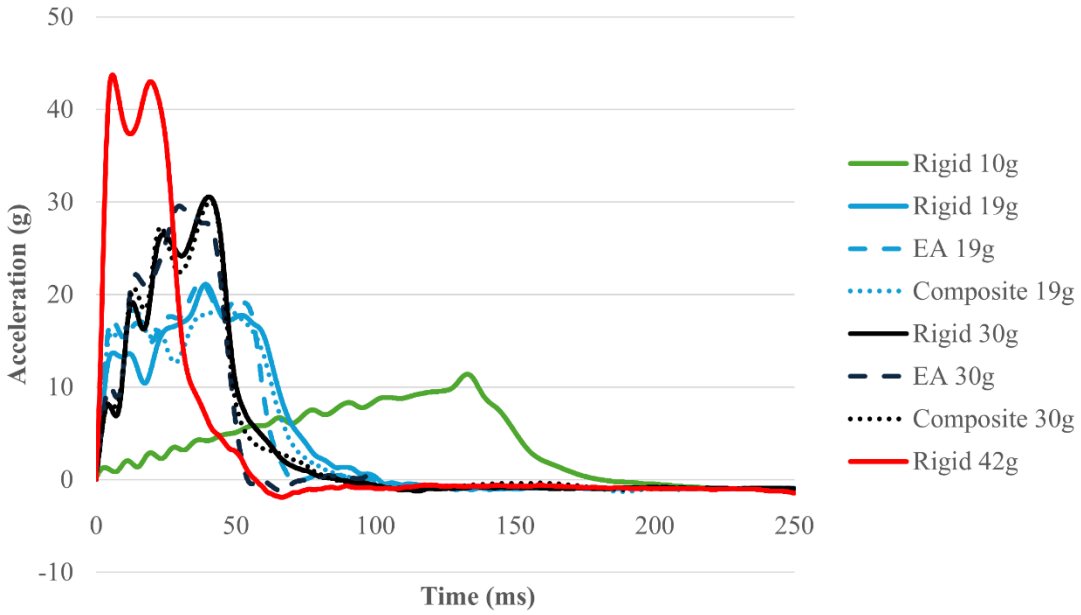

Figure 18 The crash acceleration pulses implemented in this study.

The seat models were developed and validated through component testing to characterize material models for the seat models. Each crash pulse condition was validated through comparisons of test data from the physical Hybrid III drop tower tests and simulations performed utilizing the LSTC Hybrid III 50th version 151214_BETA FEM [60]. To quantify the level of correlation between test and simulation, the ISO 18571 rating system was used and implemented using CORAplus software [61]. The ISO 18571 rating consists of a combination of corridors, a measure of how well a curve stays within a defined tolerance band of the other curve and a cross-correlation (signal similarity) comparison made between the two compared reference curves [62]. The correlation between the two curves is scored on a scale between 0

(no correlation) and 1 (exact match). A score of at least 0.5 was considered an adequate prediction of ATD response for the comparisons made between the seat test and simulation results. These scores were calculated across 10 channels of acceleration, force, and moment data including head, chest, pelvis, spine, and neck responses. All occupant response comparisons were performed between the modeled data for this study. The physical test data were only utilized for model validation in this study.

Occupant Models and Posture:

The GHBMC male 50th percentile occupant detailed model (v6.1) [51] and THOR occupant model (v2.1) [31] were selected to be used in the simulation of the vertical seat drop tests. The models were positioned to represent the position of the ATD used in the testing. This position corresponds to an approximate 90° knee and 90° hip, which allowed the feet to be in contact with the floor and arms contained within the seat geometry's bounds (Figure 20). Initial positioning of the Hybrid III and THOR models were performed using the model positioning tools included in LS-Dyna (Figure 20b-c). Similarly, the ANSA Beta tool was used for initial positioning of the GHBMC model (Figure 20d). The final position was obtained by a settling simulation that included three positioning actions. The first feature of the settling/positioning simulation was the settling by applying the acceleration of gravity to settle the HBM into the rigid seat model. Secondly, to contain the arms of the models within the bounds of a seat a single marionette pulley was attached to each distal end of the humerus representation in each model. These pulleys resulted in slight internal rotation of the shoulder.

Finally, retraction of the seatbelt elements then finalized the upright position and created the tightened position of the seatbelt for the crash simulations (Figure 20).

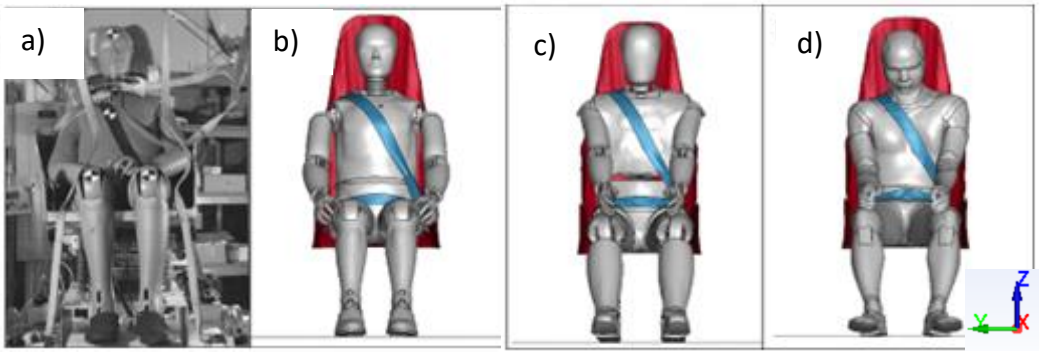

Figure 19 a) Physical ATD position and b) model positions for Hybrid III, c) THOR III and d) GHBMC.

In addition to the standard position (pelvic tilt of 40°), the GHBMC was simulated in two alternate postures related to pelvic tilt of 28 degrees, and 56 degrees which corresponds to relaxed standard and upright sitting postures, according to underbody blast loading studies (Figure 21) [63]. To achieve the alternate positions, the GHBMC standard model was modified 12 degrees lumbar flexion and 16 degrees lumbar extension utilizing the ANSA Beta tool to get the extended lumbar GHBMC (GHBMC Upright Position) and the flexed lumbar GHBMC (GHBMC Relaxed Position). While this does not achieve the same pelvic tilt, the relative tilt to the lumbar spine was used because these postures were deemed reasonable for an occupant to exhibit. The same settling procedure was performed on these models, except that the models' spinal curvature and pelvic position were constrained in the XY direction to maintain their alternate positions during the settling simulations.

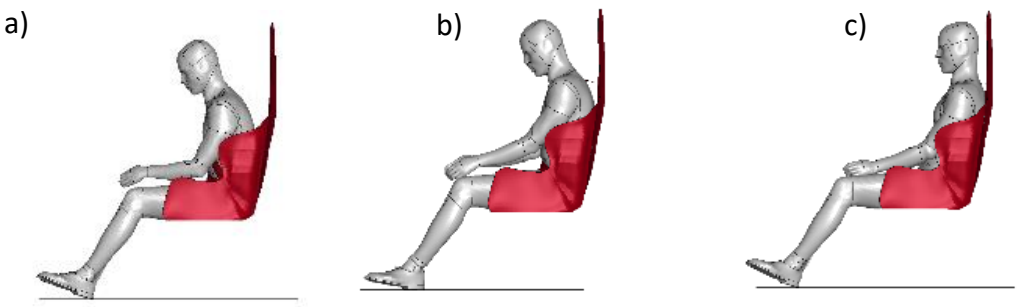

Figure 20 Initial positions of the GHBMC models: a) Relaxed position, b) Standard position, c) Upright position

Injury Calculations:

The calculations for head injuries utilized the acceleration measured at the center of gravity (CG) of the head for each occupant surrogate configuration. The instrumentation available for the neck and lumbar vertebra are different between the Hybrid III, THOR, and GHBMC. The instrumentation of the GHBMC utilizes a cross-sectional force/strain measurement at the C2 and L5 vertebrae. The strain of the THOR model utilizes outputs from a beam strain measurement at the occipital condyle (OC) joint and lumbar loadcell location on the THOR model. The Hybrid III model utilizes a beam strain output at the OC joint and lumbar loadcell location.

The injury risk metric calculated as part of this study included the head injury criteria (HIC15) and neck injury criteria (N_{ij}) metrics. HIC_{15} is the standard head injury criterion for motor vehicle safety calculated utilizing the resultant head acceleration at its center of gravity [64]. Calculations for HIC_{15} are performed as the integral of acceleration over a 15ms time interval such as:

$$\mathrm{HIC}_{15} = 15\left(\frac{1}{15}\int_{t1}^{t2} a(t)dt\right)^{2.5}$$

N_{ij} is used to characterize injury risk within the cervical spine. The injury metric was developed using piglet test data which was scaled to human anthropometry (Ref. 23). The calculations utilize critical intercepts (F_{int} and M_{int}) to normalize force (F_z) and moments (M_y) measured at the OC joint and then linearly sums the two measures as:

$$N_{ij} = \frac{F_z}{F_{int}} + \frac{M_y}{M_{int}}$$

To evaluate relative spinal loading risk predicted by each occupant surrogate, the axial force at the lumbar L5 joint was extracted and compared for all models. All data outputs were filtered to SAE CFC 108 prior to injury metric calculations to remove noise occurring in the simulations.

Results and Discussion:

Validation of Test Environment:

The seat FE models were validated through a direct comparison between the results recorded in the FE simulations of Hybrid III virtual drop tests with the corresponding data recorded in Hybrid III physical tests.

The correlation values are strongest in the vertical Z direction (Table 5). All channels in the vertical Z direction report a correlation score over the 0.5 threshold except for the 30 g rigid seat head acceleration. This is unsurprising as the loading conditions are all

implemented in the vertical Z direction. Furthermore, the movement of the extremities depends on initial model positioning.

Table 5 FEM Simulation ISO Correlation Scores

Pulse	Head AX	Head AZ	Chest AX	Chest AZ	Pelvis AX	Pelvis AZ	Spine FZ	Neck FX	Neck FZ	Neck MY
	Rigid Seat									
10g	0.256	0.713	0.466	0.676	0.734	0.768	0.793	0.235	0.674	0.238
19g	0.193	0.563	0.257	0.67	0.544	0.688	0.741	0.153	0.568	0.242
30g	0.159	0.263	0.137	0.599	0.529	0.505	0.69	0.152	0.284	0.131
42g	0.13	0.61	0.148	0.693	0.504	0.625	0.722	0.11	0.592	0.106
	EA Seat									
19g	0.07	0.594	0.485	0.666	0.426	0.639	0.662	N/A	N/A	N/A
30g	0.078	0.656	0.375	0.73	0.408	0.692	0.694	0.126	0.657	0.379
	Composite Seat									
19g	0.372	0.723	0.305	0.714	0.616	0.675	0.678	0.198	0.718	0.401
30g	0.208	0.758	0.186	0.75	0.678	0.595	0.79	0.268	0.761	0.484

Signals with scores above 0.5 are shaded.

Example plots showing this comparison with corresponding ISO 18571 rating scores above and below the 0.5 threshold are shown below (Figure 22).

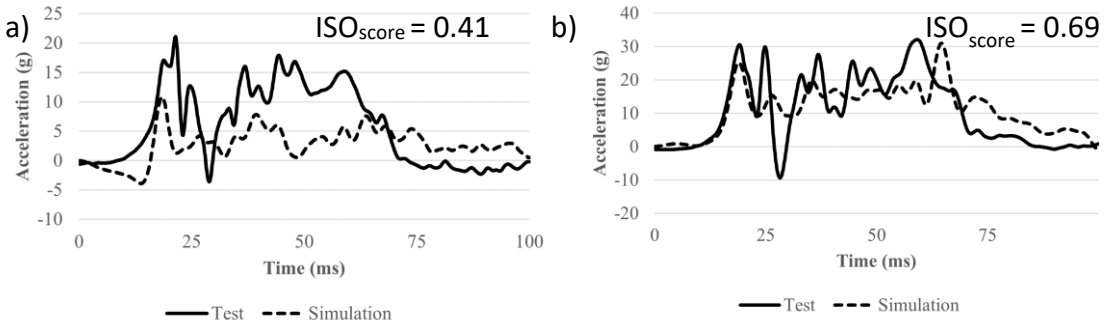

Figure 21 a) EA seat 30g pelvis AX correlation b) EA seat 30g pelvis AZ correlation

For the test conditions simulated in this study the load into the occupant surrogate is driven exclusively by vertical acceleration. Responses along this primary loading axis were all effectively predicted by the FE model, while the off-axis responses were not well predicted as they were not excited by the impact event and thus more susceptible to test variable effects such as positioning. The injury metrics evaluated are primarily driven by the vertical response in the tested conditions and thus the higher degree of error in horizontal response was not considered for the purposes of this study.

Occupant Influence:

Head Injury Metrics:

All three occupants showed increased HIC_{15} values when the magnitude of the impact pulse was increased in the four rigid seat tests (Figure 23). The relative magnitudes of the models are consistent for the lowest three rigid seat pulses with the GHBMC reporting the highest HIC_{15} values and the Hybrid III reporting the lowest. At the highest impact pulse (42 g pulse), THOR reported the highest HIC value and GHBMC the lowest.

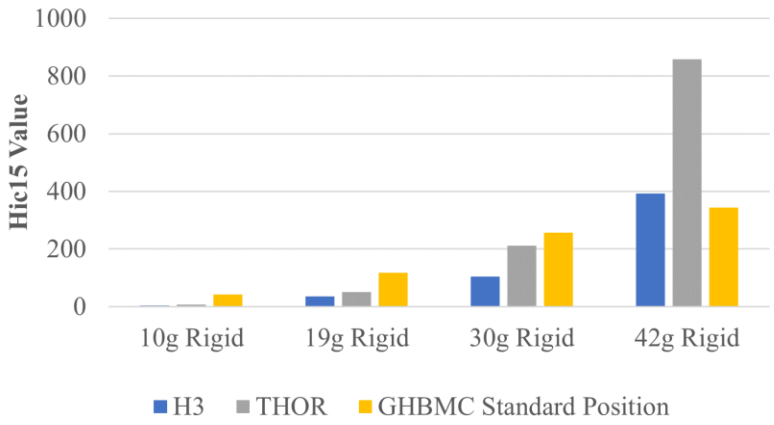

Figure 22 HIC_{15} values reported for the standard position occupants in the rigid seats.

Overall, the reported HIC_{15} values of under 400 in most of the simulated test cases would not raise concern for occupant safety (2.42% probability of AIS 3+ injury). However, the high HIC_{15} value recorded by the THOR model in the 42 g pulse alludes to some potential for head injury in this condition. In the highest pulse test (42 g), the THOR model reported the highest HIC_{15} value with a peak resultant acceleration of about 120 g at 25 ms (Figure 24). The GHBMC reports a smaller peak of approximately 65 g for close to 10 ms from 25-35 ms while Hybrid III test reported an earlier peak of approximately 90 g at 15 ms.

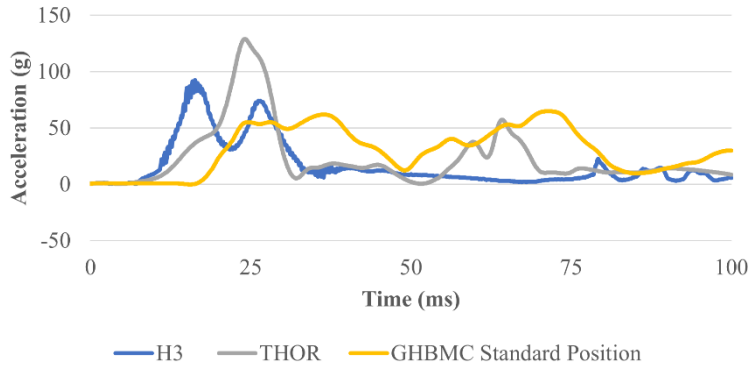

Figure 23 Time histories of head resultant acceleration in the 42g rigid seat test condition.

The difference in response to the 42 g pulse is related to the compliance of the neck from each model. The neck of the THOR model is more rigid than the neck of the GHBMC model. In addition, initial positioning of the GHBMC model allows more dampening of acceleration through the neck. The THOR head is upright at 25 ms transferring all vertical acceleration through the neck into the head without a significant rotation (Figure 25a). In contrast, the GHBMC head is beginning to tilt forward (Figure 25b), so a rotational component is added at the center of gravity of the head. This rotational component creates accelerations in the downward (-Z) direction. The primary acceleration of these models is in the upward (+Z) direction therefore this rotational acceleration lowers the total acceleration experienced by the GHBMC head. The highest HIC value is expected from the Hybrid III since it has a stiffer neck than both the THOR and the GHBMC model. The THOR model begins to respond as expected with a less steep acceleration peak up to 25 ms. However, at 25 ms the chin area of the THOR model impacts the neck components of the model. This contact between the THOR chin and neck results in a direct transfer of impact energy into the head resulting in the large spike in head acceleration measured in THOR in this condition.

a) b)

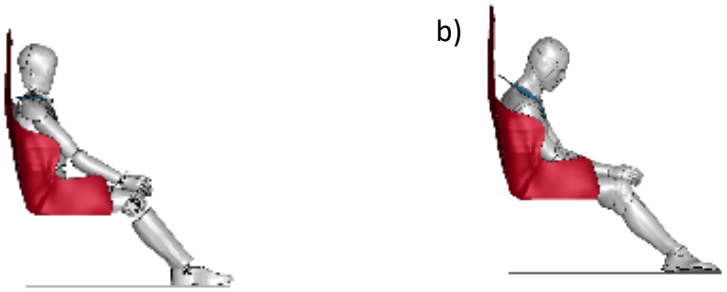

Figure 24 Occupant position at peak HIC value for the 42g rigid seat test condition a) THOR, b) GHBMC Standard Position

Neck Injury Metrics:

The GHBMC model reported the highest N_{ij} value in three out of the four crash pulses (Figure 26). All three occupants reported a consistent association between pulse magnitude and N_{ij}. The GHBMC reported higher N_{ij} value than the ATDs under the 10 g crash pulse. In addition, the Hybrid III model reported the highest N_{ij} response in the 40 g crash pulse. These data points allude to a sensitivity to pulse duration causing differing responses to the longer 10 g pulse and shorter 42 g pulse among the occupants. A cause of higher N_{ij} in GHBMC is related to its neck being less stiff than the ATD models which resulted in higher deformation during the impact.

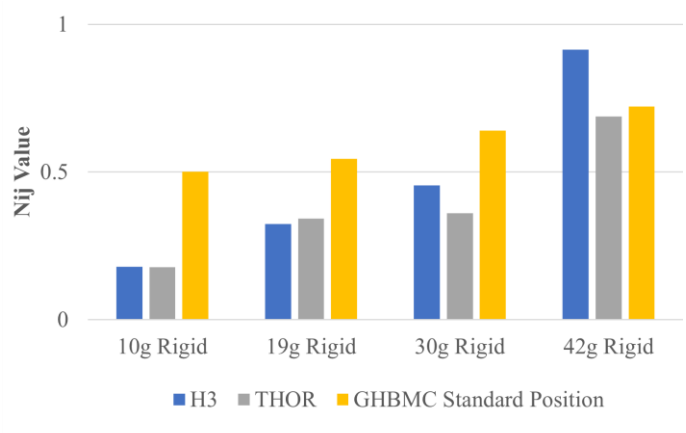

Figure 25 N_{ij} maximum values for the standard position occupants in the rigid seats.

Further evaluation of the 10 g pulse responses shows similar neck force and moment morphology that roughly follows the shape of the acceleration pulse for the Hybrid III test and THOR simulation. However, the GHBMC reported large amounts of vertical tension (Z) force and sagittal (Y) moments towards the end of the simulation (Figure 27).

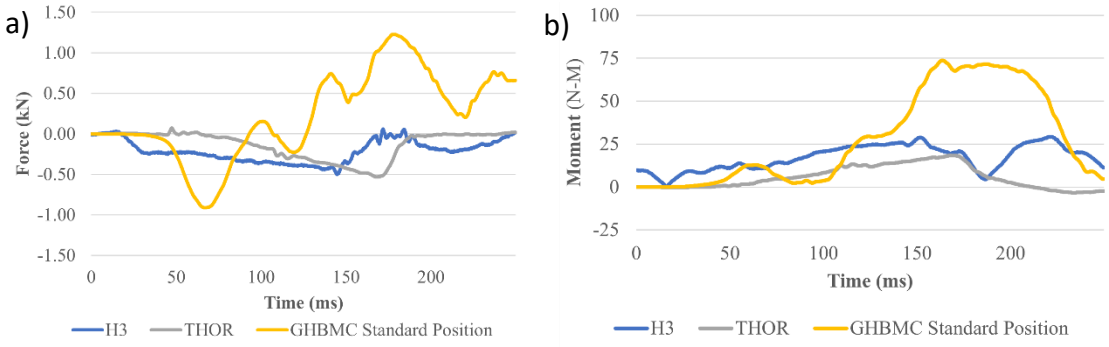

Figure 26 Time histories of N_{ij} components (rigid seat 10g pulse). a) Axial force b) Sagittal moment.

The large vertical tension force and sagittal moments reported by the GHBMC is caused by the neck structure of the GHBMC not having a muscle activation defined compared to the THOR and Hybrid III being modeled based on an active response. While 10 g is the lowest peak

acceleration condition evaluated, the pulse duration was much longer in this test compared to the others. The compliance in the GHBMC neck structure resulted in much more flexion of the neck compared to the ATDs (Figure 28). Thus, less input acceleration is required to induce neck motion and the forces and moment within the neck can build up over a longer pulse duration, compared to the more rigid ATD designs. The prediction of greater neck injury risk during longer duration loading cases by the GHBMC is an important result as it indicates that ATD's with stiffer neck structures may report neck injury risk in these conditions. However, the GHBMC results do not consider any muscle activation which could change the results. Future studies should investigate the influence of muscle activation in HBMs in these load cases.

a) b)

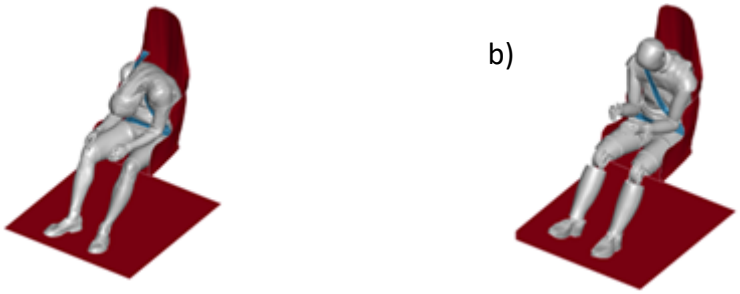

Figure 27 Occupant during rigid seat 10g FE simulation. a) GHBMC, b) THOR

In the shorter 42 g crash pulse (~100 ms vs. 250 ms in 10 g pulse), the axial force and sagittal moment morphology appears different for each of the three occupants. The Hybrid III model had the earliest compressive force response with the highest magnitude peak of around 4 kN (Figure 29a). The Hybrid III model reported the highest and longest flexion moment with reported moments over 50 N-m from about 25-55 ms (figure 29b).

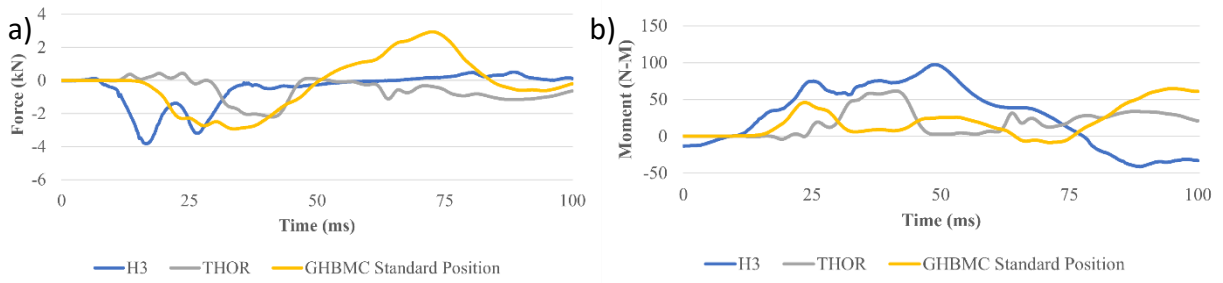

Figure 28 N_{ij} component graphs in rigid seat 42g pulse. a) Axial force b) Sagittal moment

Biomechanically, there was no difference in response from the THOR model compared to the other models for this pulse condition. However, the distribution of forces within each model creates discrepancies in the shorter pulse durations. The high magnitude of this crash pulse exacerbates the discrepancies between the models. Hybrid III appears to immediately reach maximum axial force coinciding with the peak of the acceleration pulse. This is likely due to the Hybrid III neck which is the stiffest neck of the three occupant surrogates evaluated. Increased compliance within the spinal structure of the THOR and GHBMC result in a slower buildup of axial force within the neck. The GHBMC, which contains the most deformable spinal structure of the three occupant surrogates, produces a dampened sagittal moment in the shorter acceleration pulses.

The high N_{ij} response of the GHBMC model in the 10 g pulse further supports the pulse duration sensitivity of the GHBMC model observed in the HIC_{15} response. ATDs appear to be insensitive to the pulse duration, while the GHBMC appears to be less sensitive to peak acceleration but exhibits higher relative loading in the long duration pulse conditions and lower relative loading in the short duration pulses.

Due to the higher deformability of the GHBMC neck and torso, a much higher lateral excursion of the head is observed in all simulations when compared to the ATD response. This increased lateral deformation of the upper torso and neck of the GHBMC increases N_{ij} metric values recorded by this occupant surrogate. A potential safety feature to reduce this lateral deformation is a four-point harness-type seatbelt which may decrease the lateral movement of the upper torso and neck. This potential restraint mechanism for injury risk mitigation would not have been identified using traditional ATD evaluation and thus highlights the value of HBMs to better characterize and improve occupant safety. However, more investigation would need to be carried out into other potential injury mechanisms that could be introduced by this system before its implementation.

Spine Injury Metrics:

The highest lumbar injury risk for all four datasets was associated with the highest acceleration pulse. Lumbar forces showed similar trends between the occupant models and the physical Hybrid III test data (Figure 30). The magnitude of force was consistent with the magnitude of acceleration pulse for all occupant conditions.

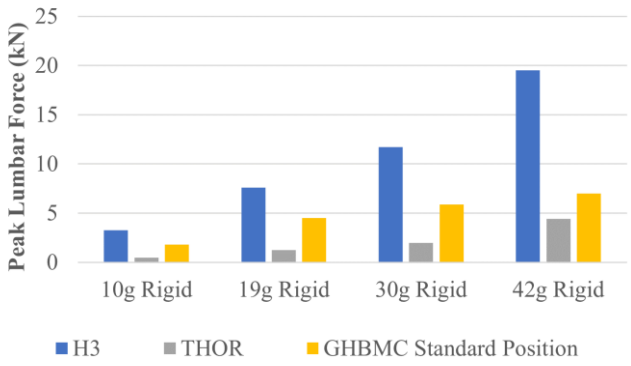

Figure 29 Peak lumbar force values reported for the standard position occupants in the rigid seats.

The GHBMC lumbar forces follow the same trends as seen in the Hybrid III testing. Both occupant surrogates showed the highest loading in the 42 g pulse condition. However, a clear difference in the magnitude of force measured from each of the occupant surrogates can be observed. In the case of GHBMC, the abdominal organs included in this human model, and which are missing in ATDs (e.g. internal organs, fat, muscle, etc.), appear to increase the distribution of forces away from the spine creating lower spinal loading. The vertical compression of the abdomen is unique to the GHBMC model due to the large number of deformable abdominal muscles and parts included in the model (Figure 31). Comparatively, compression of the thorax is more limited in the ATDs.

Figure 30 Abdominal compression of GHBMC model in 42g crash pulse

The THOR model produced lower spinal forces in all test conditions. This model had similar biomechanical compression of the spine compared to the Hybrid III, however the recorded forces were much lower. This difference between the Hybrid III and THOR lumbar loading agrees with previous physical testing of the THOR and Hybrid III ATDs in which the THOR had been seen to produce lower spinal forces due to the increased thoracic stiffness when compared to the Hybrid III model [14]. The previous testing referenced was conducted to represent frontal car crash impacts and is difficult to translate to these unique vertical loading situations. Physical comparison of THOR response in these environments would be necessary to further explore this result.

Posture Influence:

Head Injury Metrics:

Posture variation in the GHBMC model did not appear to have substantial effects on the HIC_{15} values across the pulse magnitudes evaluated (Figure 32). However, relative magnitudes

between the three occupant positions showed slight variations for the same impact pulse. The upright position exhibited the highest HIC_{15} value in the 42 g pulse and the lowest HIC_{15} in the three lower pulses. The standard position resulted in higher HIC_{15} values than the other positions in the remaining pulse conditions. The relaxed posture produced the lowest HIC_{15} values in the 42 g pulse and produced middle values in the other three conditions.

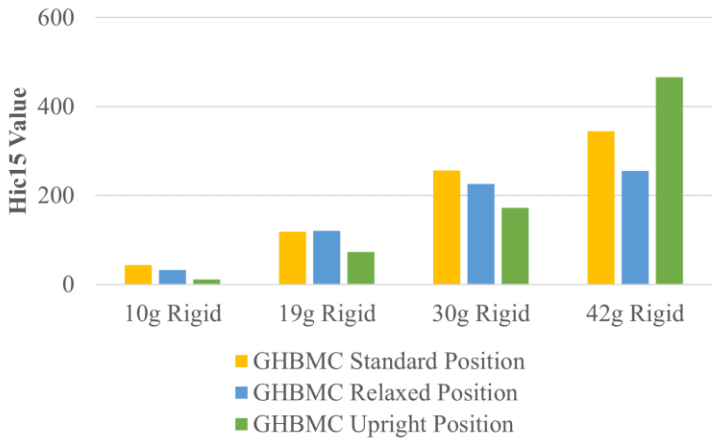

Figure 31 HIC_{15} values reported for the varied positioned GHBMCs in the rigid seats.

Biomechanical differences resulting from positioning help us better understand the mechanisms that can lead to head injury in this type of impact environment. The upright GHBMC maintains an upright head/neck position at the time of peak acceleration of 25 ms (Figure 33). Similarly, to the THOR model, this produces a direct vertical acceleration path through the neck of the occupant during peak load resulting in increased vertical acceleration measured at the head.

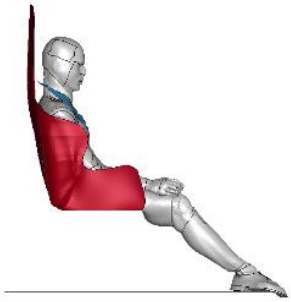

Figure 32 Position of upright GHBMC at occurrence of max HIC in rigid seat 42g pulse.

For the cases evaluated the reduction in head injury risk due to posture was minimal as all conditions produced values below injury metric limits, however understanding the effects of posture on head acceleration loading may allow for future development of safety features to ensure safety at more severe impacts. While the upright position reported the lowest HIC_{15} values in three out of the four crash pulses, it should be viewed as the most dangerous posture for head injuries as it is clearly reported to produce higher injury risk at higher crash pulse magnitudes. The safety technique of bracing forward as seen in plane crashes may be beneficial to adapt for eVTOL occupants due to the potential decrease in head injury risk in more severe crash conditions.

Neck Injury Metrics:

There was a slight variation of N_{ij} values between the GHBMC positions (Figure 34). In the 42g pulse the neck response of the upright GHBMC reported the highest N_{ij} value for all rigid seat occupant pulse combinations. N_{ij} values increased with the magnitude of acceleration pulse in all positions. In the 10 g pulse, the upright GHBMC reports a substantially lower N_{ij} value, which was in line with the values measured in the ATD occupants for this condition.

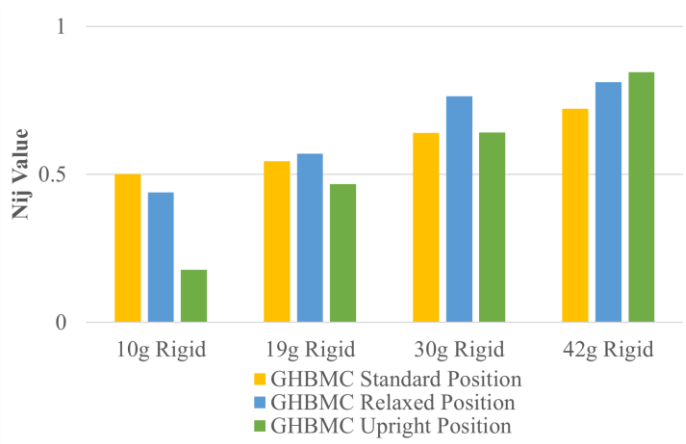

Figure 33 N_{ij} values reported for the varied positioned GHBMCs in the rigid seats.

The position of the upright GHBMC creates responses like the ATDs evaluated. In the longer 10 g pulse, the upright GHBMC does not reach peak neck deformation until the very end of the 250 ms pulse (Figure 35a). The standard position reaches a greater max deformation at 175 ms (Figure 35b). The upright position of the GHBMC creates a stiffer neck response leading to both a larger axial force and sagittal moment measurements early in the simulation (Figure 36). In addition, the upright position reports the neck in compression for a longer duration during this crash condition. This is due to the higher deformation necessary to rotate the neck into tension loading.

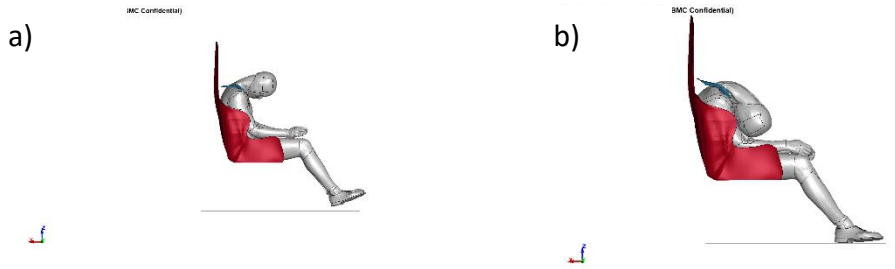

Figure 34 Maximum neck deformation in rigid seat 42g condition. a) Upright GHBMC b) Standard GHBMC

Figure 35 Rigid seat 10g pulse Nij component graphs for GHBMC alternate positions. a) Axial force, b) Sagittal moment.

The N_{ij} results from the varied positioned GHBMCs shows the limitations of the ATD (THOR and Hybrid III) models to represent the human body. It is apparent that the more rigid spinal components of the ATD models result in similar trends to the GHBMC model positioned with a more upright lumbar angle. However, the human body is not as rigid as the ATDs and therefore the complete upright neck posture is not necessarily representative of the biodynamics a human would experience in these crash environments. Furthermore, the

utilization of the ATDs may overreport or underreport injury risks in lower magnitude crash pulses. Positional variations in a real crash event are not possible to fully control so safety features which account for potential variations in posture are important. Studies of these posture variations are not feasible with current ATD designs and therefore the GHBMC proves to be a useful tool for evaluating neck injury risk that may depend on posture.

Spine Injury Metrics:

The relaxed position resulted in the lowest spinal force in all four rigid seat pulse conditions (Figure 37). In addition, all three positions associated the magnitude of lumbar force with the magnitude of crash pulse acceleration.

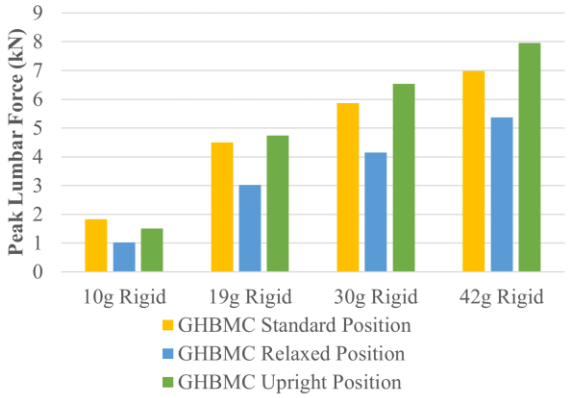

Figure 36 Max spinal force values reported for the varied positioned GHBMCs in the rigid seats.

The biomechanical deformation of the relaxed position is the most substantial out of all three positions (Figure 38). This thoracic deformation in the relaxed posture results in more significant offloading of spinal forces into the deformable abdominal parts reducing lumbar load. This effect is seen in all impact pulses evaluated and further supports the hypothesis that reduced lumbar loads measured in the GHBMC compared to the ATDs is a result of the

increased thoracic deformation and energy absorption through the abdominal tissues in the GHBMC.

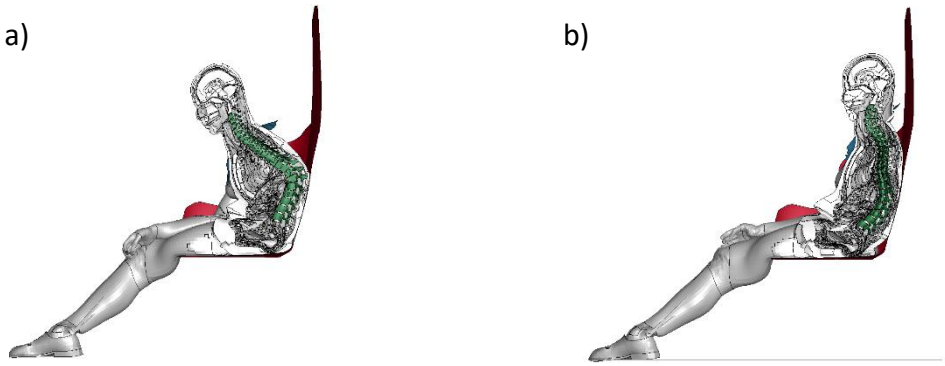

Figure 37 Maximum thoracic deformation in rigid seat 42g condition. a) Relaxed GHBMC b) Upright GHBMC

All three positions report similar trends associated with pulse magnitude for peak lumbar force. These trends remain in agreement with the trends reported by the ATD models. Similar to head injury, it is apparent that the upright posture produces the highest injury risk as it reports the highest peak lumbar force values. Hence, further testing and safety feature development may target this position for improving safety. The relaxed positioning allows the dampening of lumbar forces away from the spine. Results presented from the spine and head injury study allude to the fact that this may be the safest of the three postures to assume in the event of a crash. However, further evaluation is necessary to concretely determine safety due to injuries not expressed by the injury metrics in this study such as bending moment on the spine. Future studies may benefit from incorporating alternative injury assessment criteria such as Brinkey injury criteria.

Seat Influence:

Each occupant in the standard pre-crash posture was analyzed to compare relative injury metric magnitude across the three seats tested in the 19 and 30 g pulses. Each combination of occupant, pulse, and injury metric (HIC_{15}, N_{ij} and peak lumbar force) resulted in a seat associated with lowest, middle, and highest injury metric reported. The EA seat was associated with the lowest injury metric for the majority (32/36) of occupant model, pulse and injury metric combinations. There were four cases of low rankings of seat injury association not in the EA seat. THOR neck injury reported the lowest injury risk in the composite seat and the rigid seat for the 19 g and 30 g pulse respectively. The GHBMC reported the lowest neck injury risk in the rigid seat during the 19 g pulse. The GHBMC in the upright position reported the lowest spinal injury risk in the composite seat during the 19 g pulse.

Head Injury Metrics:

The lowest head injury values for all pulse and seat combinations evaluated were associated with the EA seat (Figure 39). The composite seat increased risk in 8/10 pulse occupant combinations compared to the rigid seat. The standard and relaxed GHBMC 30 g pulse were the only two cases that saw a reduction in HIC when implementing the composite seat (Figure 39b).

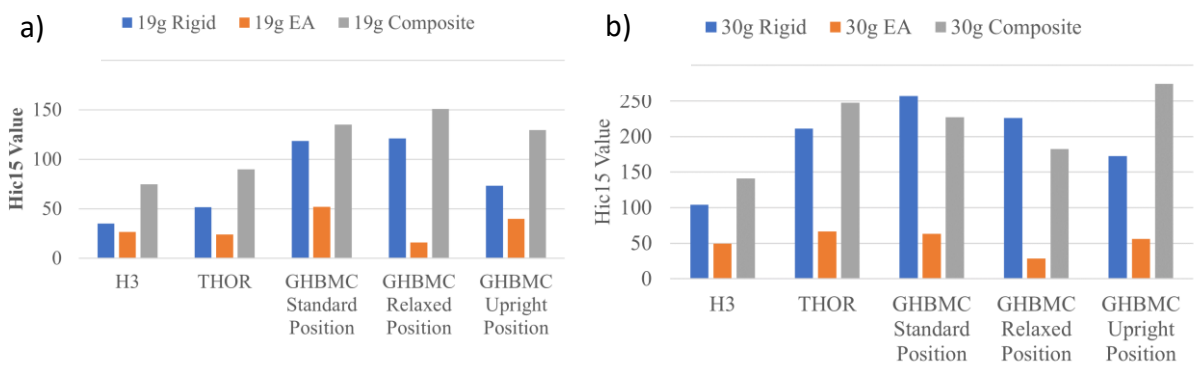

Figure 38 HIC_{15} values across the three seat models for each occupant. a)19g pulse b) 30g pulse

Comparing the GHBMC Standard position response in the 19 g and 30 g crash pulses can illuminate the differing responses to the composite seat reported by the standard and relaxed position. Both the EA and composite seats reduce HIC_{15} value by reducing the magnitude of the initial head acceleration peak (Figure 40). Towards the end of the simulation, the composite seat produced the highest maximum mangitude of acceleration in both the 19 and 30g pulses. However, in the 30g pulse, the duration of this peak is too short in duration to yield a higher HIC_{15} value. Biomechanically this secondary peak occurs due to the flexible nature of the composite seat. Initially, the flexion dampens the acceleration and reaches max flexion around 60 ms (Figure 41a). The rebound force then creates a whiplash effect beginning around 80 ms when the secondary peak begins (Figure 41b). The shortening of the secondary peak in the 30 g pulse may be due to a combination of neck position at occurence of this whiplash effect and the slighly shorter duration of the crash pulse itself.

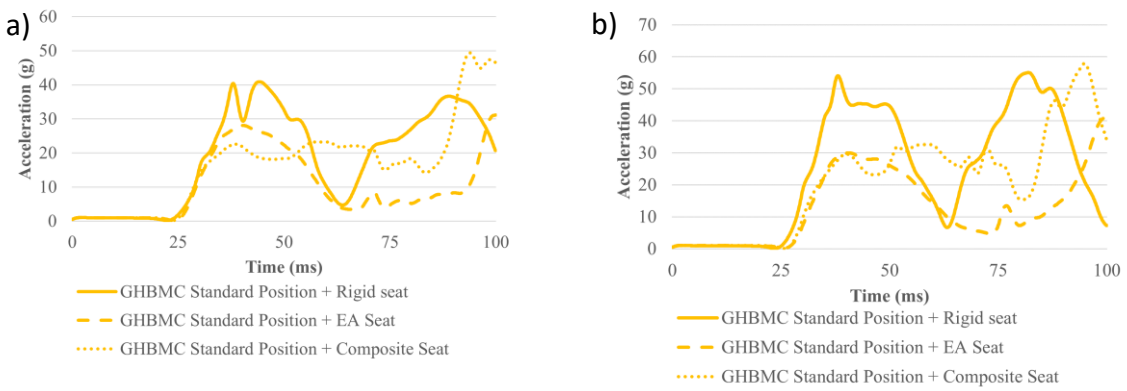

Figure 39 Resultant head acceleration values across the three seat models for the standard positioned GHBMC. a)19g pulse b) 30g pulse

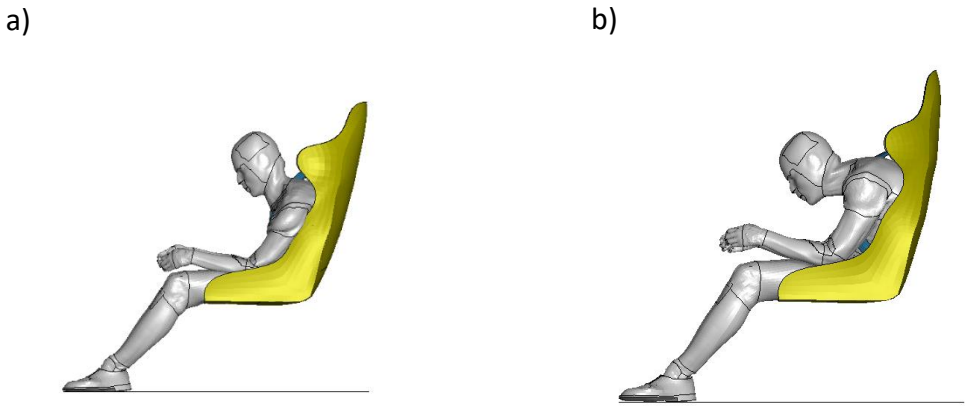

Figure 40 GHBMC position during 19 g composite seat crash condition a) 60 ms b) 80 ms

Similar to how the composite seat flexes in the horizontal direction to dampen the innitial peaks of acceleration, the EA seat dampens in the vertical direction through the compression of the EA tubes. However, the EA tubes remain compressed instead of rebounding to their original position (Figure 42). There still appears to be a secondary peak due to the forces created when the EA tubes bottom out but the magnitude of the effect is lower than that of the composite seat.

Figure 41 Position of GHBMC standard position at 80 ms of EA seat 19 g crash condition

Neck Injury Metrics:

The reported N_{ij} metrics across the seat models utilized reported the EA seat as the lowest injury risk seat in 7/10 pulse-occupant combinations. Two of the cases that reported lower N_{ij} for a different seat were both associated with the THOR model. In the 19 g pulse, the THOR model produced the lowest Nij value in the composite seat (Figure 43a). However, in the 30 g pulse the THOR model produced the lowest N_{ij} value in the rigid seat (Figure 43b). The final case that reported lower Nij for a different seat is the GHBMC upright position in the 19 g pulse.

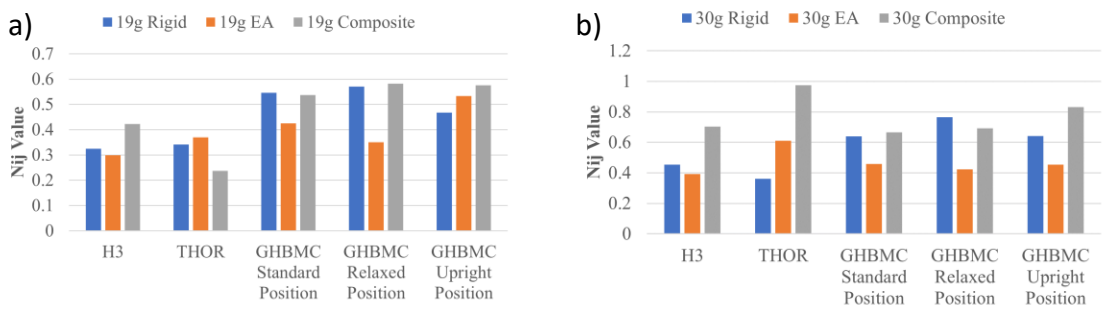

Figure 42 N_{ij} values across the three seat models for each occupant a) 19 g pulse, b) 30 g pulse

The 30 g pulse THOR condition resulted in the highest variation of N_{ij} value. The lowest value, of under 0.5, was associated with the rigid and the highest was associated with the composite seat with a N_{ij} value of almost 1. There are large spikes after 25 ms in both response components within the EA and composite seat conditions (Figure 44). At 25 ms directly before the peak, there is no distinguishable difference in the positioning of the THOR model (Figure 45). It is possible that at this timestep slight differences in seat interactions create these spikes. However, there are no clear biomechanical differences which would simply explain this spike. Therefore, it is most likely that this is a computational and or instrumentation issue with the THOR model.

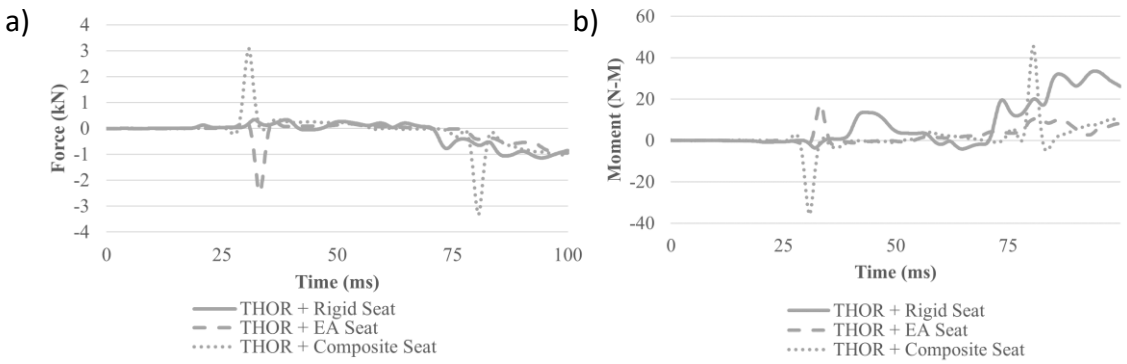

Figure 43 30g pulse Nij component graphs for the THOR model in all three seats. a) Axial force, b) Sagittal moment

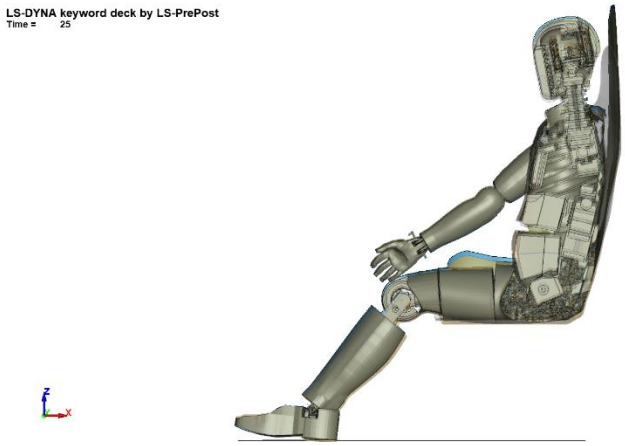

Figure 44 Overlay of all three 30g THOR models at 25ms

The Upright GHBMC N_{ij} response in the 19 g pulse reports very similar component responses across the seat types for most of the simulation (Figure 46). However, at the end of the simulation the EA seat reports a substantial extension moment. The initial dampening by the EA tubes reduces the deformation of the GHBMC neck which initially decreases both components of N_{ij} calculations. This reduced deformation leads to a higher extension moment

when the EA tubes bottom out and create a secondary peak of neck compression. The critical intercept for extension is lower than flexion for N_{ij} calculations creating a higher injury metric for the EA seat in this case.

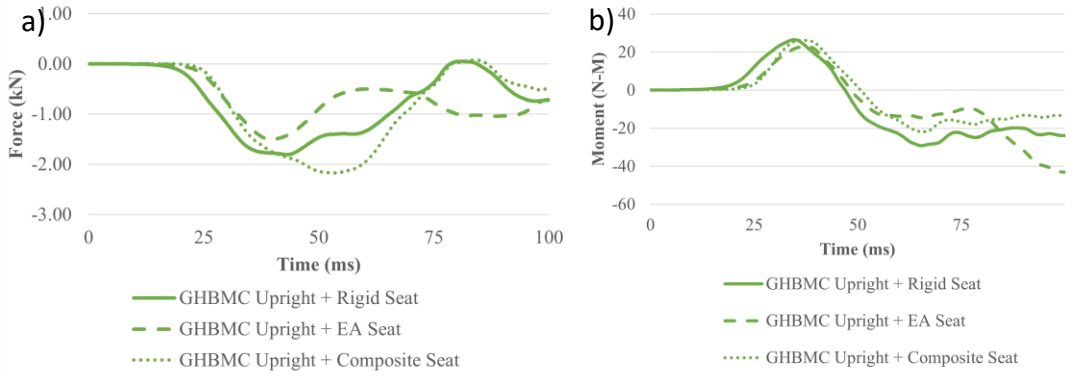

Figure 45 19g pulse Nij component graphs for the GHBMC model in all three seats. a) Axial force, b) Sagittal moment.

While there are discrepancies between the model and test data responses, no model or seat reports N_{ij} values above the standard injury threshold of 1. All the EA seat N_{ij} metrics report values at or below 0.6. The composite seat is associated with the two data points most concerning for injury with the THOR (0.97) and GHBMC Upright (0.83) in the 30 g pulse. The potential instrumentation issues identified in the THOR model require further exploration to verify the model's response in these tests. However, the mechanisms identified by the GHBMC upright condition show potential considerations of occupant position that should be accounted for in safety feature design for eVTOLs.

Spine Injury Metrics:

Once more, the EA seat showed a good injury mitigation in 9/10 of the occupant pulse combinations reporting the lowest spinal force of the seats evaluated (Figure 47). The only

exception was the GHBMC standard position that reported slightly lower axial force for the composite seat in the 19 g pulse (Figure 47a). The THOR and GHBMC model both reported substantially lower variation across the different seats compared to the Hybrid III model.

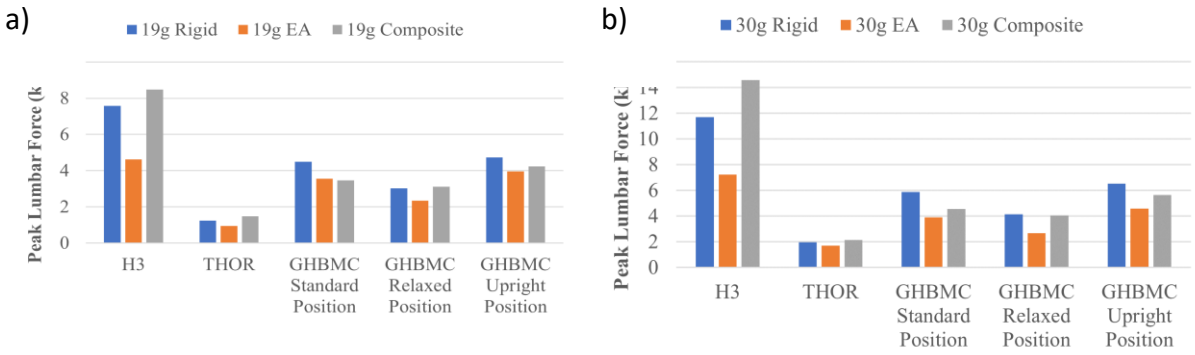

Figure 46 Peak lumbar force values across the three seat models for each occupant. a) 19g pulse, b) 30g pulse

Through analyzing the spinal loading response of the standard GHBMC, slight variations in response from the EA and composite seats can be seen. In the 19 g crash pulse the composite seat follows a similar morphology to the EA seat with both seats dampening the initial spinal loading (Figure 48a). However, in the higher acceleration pulse the dampening of the EA seat has a greater effect during the initial peak (Figure 48b). Both the EA seat and the composite seat appear to dampen the spinal loading of the models. However, the mechanisms of dampening are different for these two seats. The EA seat dampens loading specifically in the vertical (Z) direction through the compression of the EA tubes. The composite seat dampens through the reclining flexion of the seat under load, diverting some of the vertical force into horizontal bending of the seat. At the higher crash pulses, the composite seat reaches max bending and absorbs less forces than the EA seat.

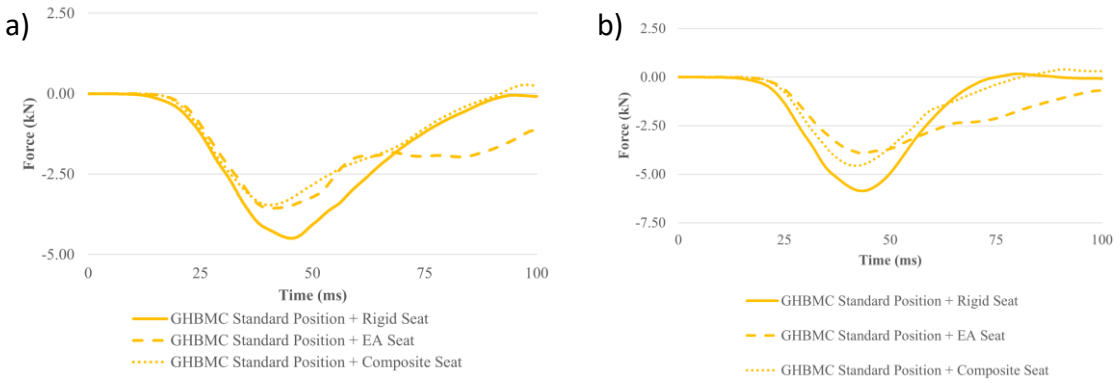

Figure 47 Lumbar force time history for GHBMC Standard position in all three seat models. a) 19g pulse, b) 30g pulse

All models agree that the EA seat produced the lowest injury metric response with respect to spinal loading. While the composite seat reports some force reduction in the more deformable GHBMC and THOR models, the rigid Hybrid III test data reports higher spinal forces within this seat. The more deformable models are assumed to be more representative of a true human body response to these loading conditions. However, the less substantial effect reported verifies the EA seat as the more protective seat option. Furthermore, the spinal loading values seen are the most concerning for potential injury in these studies. Utilizing a predictive equation, 26 out of 40 reported spinal loading values are associated with at least 5% risk of spinal fracture (over 3.2 kN loading) [66]. Therefore, with most occupant simulations producing reduced injury risk within the EA seat, especially at higher impact pulses, the EA seat was determined to be most effective at limiting occupant injury risk among the seats studied.

Overall Assessment:

All occupants provided valuable insight into these test conditions with varying utilizations of computational resources. The GHBMC model is the most complex model,

containing millions of elements and nodes, requiring between 12-24 hours of computational runtime depending on resource allotment. The THOR and Hybrid III V-ATD models are substantially simpler, with hundreds of thousands of nodes. Due to their simplicity, they only required 4-8 hours of computational runtime. While none of the models extensively limited this study due to computational consumption, the V-ATD models do provide substantially quicker results.

The highest injury metric for all test conditions simulated was associated with the 42 g rigid seat pulse for all occupants and metrics except for the THOR N_{ij} response. The THOR reported its highest N_{ij} value associated with the 30 g composite seat. The highest HIC_{15} value was reported by the THOR 42 g rigid seat test due to the impact of the model's chin components against the occupant's neck. The largest spinal load was reported by the Hybrid III model due to its stiff spinal construction. While the GHBMC did not report any ultimate highest injury metrics, biomechanical responses illuminate potential mechanisms of injury that may be most representative of a human body.

Spinal loading is the most likely to cause injury of the risks evaluated. Both the Hic and N_{ij} values reported for all tests are not typically associated with elevated levels of injury risk. Therefore, safety features and research will typically be focused on reducing spinal loading. Currently, the standard for evaluation are Hybrid III dummies and models. These models have stiffer spines than both the GHBMC and the THOR models. Therefore, this study verified the Hybrid III higher magnitudes of spinal loading. Safety features designed to reduce spinal loading on the Hybrid III are likely to have similar effects on other dummies and models.

Continued development utilizing these models will allow for decreased injury risk on all occupants and increase safety. This was seen in the consistent trends of reduction in spinal injury associated with the EA seat. However, limitations in positioning evaluations and the varied results in the other two metrics necessitate usage of various models to draw more concrete conclusions.

Across most conditions evaluated the EA seat produced the lowest injury risk for in each of the occupant surrogate models. However, there were four exceptions to this finding with two associated with the THOR N_{ij} metric, one with the upright GHBMC N_{ij} metric, and one with standard GHBMC spinal force. There were discrepancies around the effect of the composite seat on the various occupants. Both the EA and composite seats affected the predicted injury metric responses by altering the distribution of forces through the seat constructions and the models. While this study did not identify substantial increased injury risks associated with any of the occupant's reactions to the alternate seats, more complex safety features may not benefit advanced models positively if testing is only evaluated with the Hybrid III. In addition, positional variation had recognizable effects on injury risk of which the Hybrid III is less capable of evaluating when compared to the GHBMC.

The alteration of GHBMC position identified trends across all the injury metrics. The relaxed and standard GHBMCs produced similar HIC and N_{ij} values across the conditions evaluated. However, the upright GHBMC reported injury metrics and mechanisms which were more like the ATD models. The key finding from the altered positions was the reduction in spinal force associated with the relaxed position. This relaxed position is like the bracing

technique utilized as a safety tool for airplane crash events. Seat designs to maximize this benefit would need testing or modeling that the Hybrid III or other simpler occupants may not be capable of accurately representing.

Conclusions:

It is important to put emphasis on potential mechanisms of injury reported by each occupant surrogate as each have been validated in their own ways. Each of the occupant surrogates reported the highest injury risk in at least one test condition evaluated within this study. For the ATD models, the highest injury metric values were predicted with the highest acceleration pulses regardless of pulse duration. The GHBMC model was more sensitive to pulse duration than any of the other models, especially for neck injury. The THOR model had the least consistency in injury risk reported. The relaxed GHBMC position reported a reduction in spinal forces while the upright position generally resulted in a reduction in neck injury risk similar to the ATD models. The injury risks results from each models identified potential safety feature interventions. The first is the studied energy absorption tubes that were included in this study. All models identified a reduction in spinal force when the energy absorbing seat was used as compared to the rigid seat. Second, while the injury risk was lower in the GHBMC, the sensitivity to pulse duration for 2/3 positions and the increased lateral motion of the neck and torso may necessitate research into more substantial restraint systems. eVTOL aircraft researchers may use each of these occupant surrogate tools, with a proper understanding of their capability and limitations, to analyze vehicle safety and identify potential avenues for injury risk interventions.

This study shows the value of FE modeling tools for evaluating a variety of human surrogates for crash injury reporting. Further studies can continue to implement more factors, whether in varying occupant size, new HBMs, varying crash pulses or varying model initial positions. These can all be quickly and efficiently tested to identify factors that reduce injury risk for occupants to guide development of regulations for these new vehicles.

This area of research remains limited by the validation of these models in aerospace loading environments. Further development of aerospace specific HBMs and ATDs will provide value in developing this field of research. In addition, due to the early development stage of these novel vehicles, there is great potential to integrate new mechanisms for safety within vehicle design to prevent injury. Continued research into the safety and implementation of these novel eVTOL vehicles will need to be supported by FE modeling to protect occupants in emergency situations.

Chapter 4: Expansion on Study of Advanced Occupant Models to Quantify Injury Risk for eVTOL Vehicles

Introduction, Model Simplification and Development:

This final stage of work was initially intended to be composed of full simulations of a complete eVTOL aircraft shell with the THOR and GHBMC models. The simulations were developed utilizing the full lift plus cruise (LPC) eVTOL shell with two occupants in each test (Figure 49). These models, however, were extensively complex and would require substantial computational power to complete. Consequently, this setup ran into a multitude of issues. The In–lbf–sec unit system was utilized in the development of the complex aircraft model. The aircraft consisted of multiple complex composite materials that would have been difficult to modify into the kg-mm-msec unit system in which both the GHBMC and THOR models were designed. Instead, the GHBMC and THOR model conversions were performed to run these models. However, preliminary runs of this simulation environment were unstable, with errors arising within the first 10 ms of the crash impact simulations. Iterative simplification was necessary to create stable runs of these simulations.

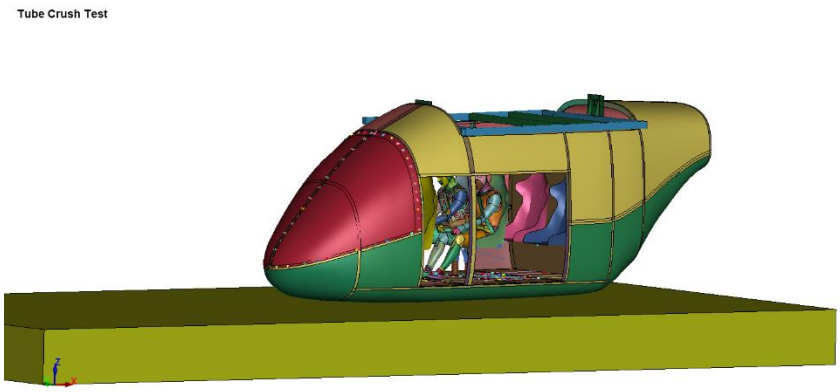

Figure 48 Full LPC model with 2 GHBMC Occupants

The first step of simplification attempted was reducing the number of occupants from 2 in each simulation to 1 in each simulation. This simplification reduced the number of complex elements in the simulation. However, instabilities continued, and consistent failures persisted in the aircraft and occupant models. These models were also plagued by frequent “exploding” elements, preventing simulations from running long enough to yield usable outputs (Figure 50). The issues were diagnosed with a combination of the converted occupant and complex vehicle models through many debugging simulations. To avoid extensive redevelopment of the occupant models, which was determined to be outside this project's scope, a breakout model was developed to successfully run and analyze occupant responses in these tests.

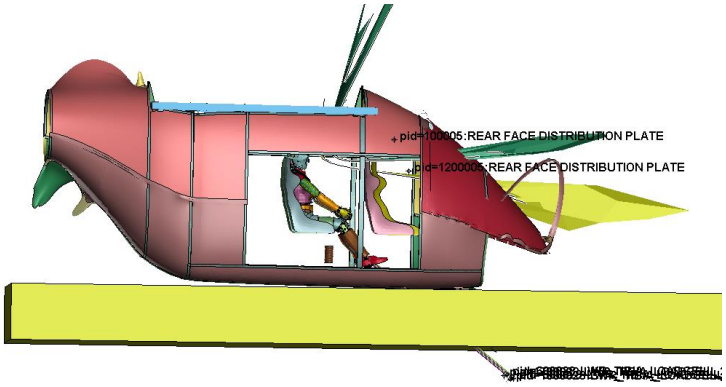

Figure 49 Full LPC model showing "exploding" elements during simulation

The breakout models utilized slightly modified seat models from the previous drop tower test (DTT) model environment. The two modeled and utilized seats were a composite and an energy-absorbing (EA) seat model. These seats correspond to the full LPC model's right (Composite) and left (EA) seats. These seat models were previously converted to the mm-kg-msec unit system to match the occupant models. The crash pulses implemented were developed through the extraction of floor-level accelerometer data. This accelerometer data was extracted from simulations of the entire model utilizing point masses to represent the later implemented occupants.

Attempts were made to run these breakout models with 6 degrees of freedom, including both x, y, and z directional acceleration and rotational velocities. The crash pulses were implemented through prescribed local boundary conditions at a coordinate system matching the relative placement of the accelerometers utilized in the crash pulse development

simulations. The increased motion resulting from the 6 degrees of freedom continued to result in instabilities with the models. While some of the GHBMC simulations were successful, the rotational velocities resulted in instabilities with mass scaling and biomechanics that appeared more violent than expected. These instabilities and uncertainties associated with implementing rotational velocities resulted in the final simplification of removing the rotational velocity boundary conditions.

The resulting 3-degree of freedom models were implemented for five crash pulses in the two-seat test conditions, utilizing the standard positioned GHBMC and THOR models. The THOR model was run first as researchers presumed the simpler ATD model would have less complicated debugging. However, preliminary trials utilizing the THOR model resulted in constant failures due to mass scaling. The central part responsible for these failures was part 700053, “Shoulder Padding R” (Figure 51).

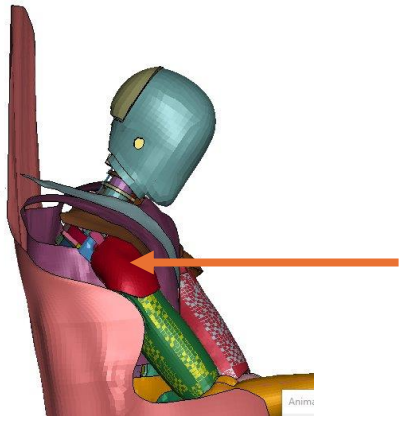

Figure 50 THOR model highlighting problematic shoulder padding part.

Multiple approaches were attempted to resolve these issues. The first and most extensive debugging solution implemented was alterations of the minimum time step for mass scaling. This solution increased the runtime from 40ms to 95ms in test pulse one. However, many simulation conditions still failed within the first 40-85ms. Other debugging approaches included redeveloping the ATD model’s contacts, adding erosion cards, and allowing mass-scaled elements to be eroded. A combination of these approaches reports the maximum runtimes achieved for the THOR model in Table 6.

Table 6 THOR error termination times.

THOR Model Run Times	EA Seat	Composite Seat
C1	95 ms	55 ms
C2	85 ms	40 ms

C3	75 ms	N/A
C4	85 ms	N/A
C5	45 ms	N/A

None of the THOR model test runtimes were to the 100ms completion criteria set by the researchers. The solutions for improving this model's stability for these simulations constituted extensive redevelopment of the THOR model. While this redevelopment would be helpful for further exploration utilizing this model, it was deemed outside the scope of this research. Therefore, the THOR simulations were removed from this study.

The researchers also implemented the relaxed and extended GHBMC positions developed in the previous DTT study to allow for sufficient data points for comparison upon removing the THOR model. The three positions of the GHBMC model were implemented in all 5 of the crash pulses provided by NASA. However, 2 of the crash pulses (C3 and C5) resulted in model instabilities. Due to these instabilities, only the C1, C2, and C4 crash pulses were completed and compared across the three positions.

Methods:

The various instabilities requiring development outside this project's scope resulted in an alternative study. The goal of this study was to achieve a similar goal of exploration of advanced occupants in a more realistic eVTOL crash environment.

This study utilized the GHBMC model in the three positions developed for the DTT simulations. The 3 GHBMC models were placed into 2-seat models. These two models were the EA and Composite seats previously evaluated (Figure 52).

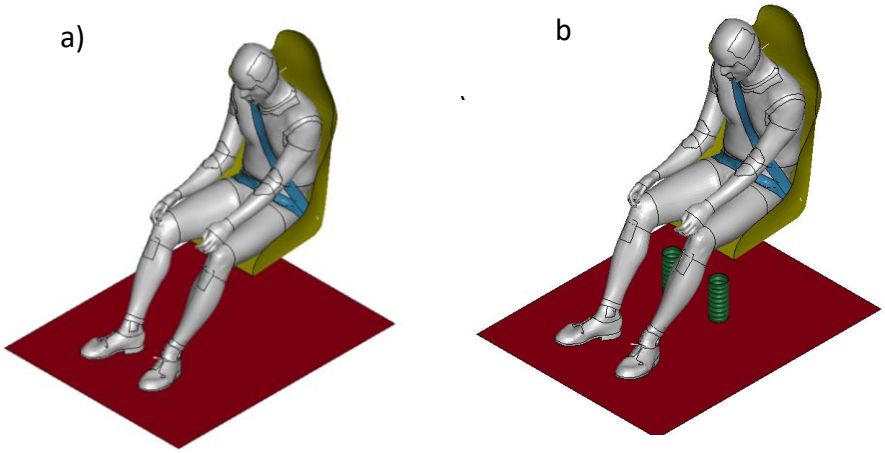

Figure 51 Breakout model with standard positioned GHBMC
a) Composite Seat
b) EA Seat

The three positions were implemented in 3 crash pulse environments for each seat, resulting in 18 simulations. These pulses will be referred to conditions 1, 2, and 3. However, these pulses represent the original crash pulses associated with tests C1, C2 and C4. These pulse conditions allowed for stable running of each of the three occupant positions. The crash pulses included prescribed accelerations in the x,y, and z directions. They were implemented using the local coordinate system developed to represent the accelerometer from which they were extracted in the full eVTOL model simulation.

This study utilized the same digital instrumentation and injury metric calculations analyzed for both previous studies. The calculations for head injuries utilized the acceleration

measured at the center of gravity (CG) of the head for each occupant surrogate configuration. The digital instrumentation of the GHBMC utilized a cross-sectional force/strain measurement at the C2 and L5 vertebrae.

The injury risk metric calculated in this study included the head injury criteria (HIC_{15}) and neck injury criteria (N_{ij}) metrics. HIC_{15} is the standard head injury criterion for motor vehicle safety calculated utilizing the head acceleration at its center of gravity. Calculations for HIC_{15} are performed as the integral of acceleration over a 15ms time interval:

$$\mathrm{HIC}_{15} = 15\left(\frac{1}{15}\int_{t1}^{t2} a(t)dt\right)^{2.5}$$

N_{ij} is used to characterize injury risk within the cervical spine. The injury metric was developed using piglet test data scaled to human anthropometry. The calculation utilizes critical intercepts to normalize force and moments measured at the OC joint and then linearly sums the two measures as:

$$N_{ij} = \frac{F_z}{F_{int}} + \frac{M_y}{M_{int}}$$

To evaluate the relative spinal loading risk predicted by each occupant surrogate, the axial force at the lumbar L5 joint was extracted and compared for all models.

Results and Discussion:

Head Injury:

All HIC values reported are not typically associated with injury. The highest HIC value reported was 545, observed in the relaxed position GHBMC from the pulse 2 test condition

(Figure 53). This HIC value was associated with only a 5.9% probability of AIS 3+ injury. The standard and upright positions reported lower HIC values for the EA seat. However, the relaxed position simulations reported lower Hic values associated with the composite seat in two test conditions. Overall, the extended position simulation reported the lowest HIC values.

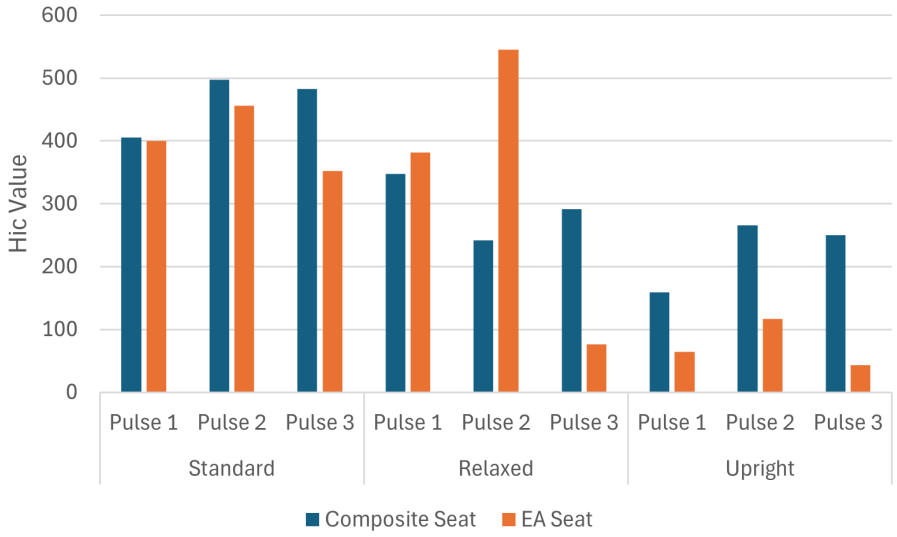

Figure 52 Hic values reported by each occupant under all test conditions.

The higher HIC values reported from the relaxed position in the Pulse 2 EA seat were due to an impact of the GHBMC head against the arm of the GHBMC (Figure 54). The higher initial lumbar flexion of this model appeared to increase the likelihood of the head impacting other elements or limbs of the model. In addition, the EA seat compression allowed the head to reach higher velocities by delaying the self-impact until later in the simulation.

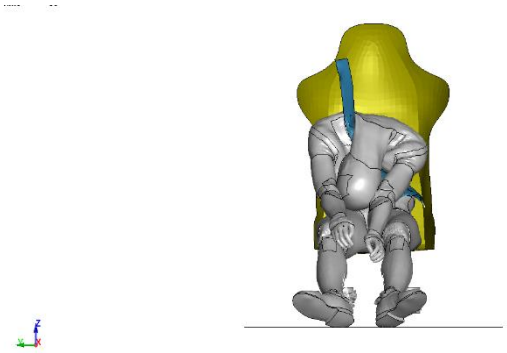

Figure 53 Head impact of relaxed GHBMC head on right arm during pulse 2 EA seat test condition.

Neck Injury:

None of the reported N_{ij} values exceeded the standard injury threshold 1 (Figure 55). The highest reported N_{ij} value was 0.91, reported by the upright GHBMC simulation under the Pulse 2 composite seat condition, with a similar value of 0.90 reported by the relaxed GHBMC under Pulse 3. The EA seat was associated with lower N_{ij} values in 6 of the nine tests. The only test that reported a somewhat substantially higher N_{ij} value related to the EA seat was the relaxed Pulse 1 test condition; however, the difference was only 0.09.

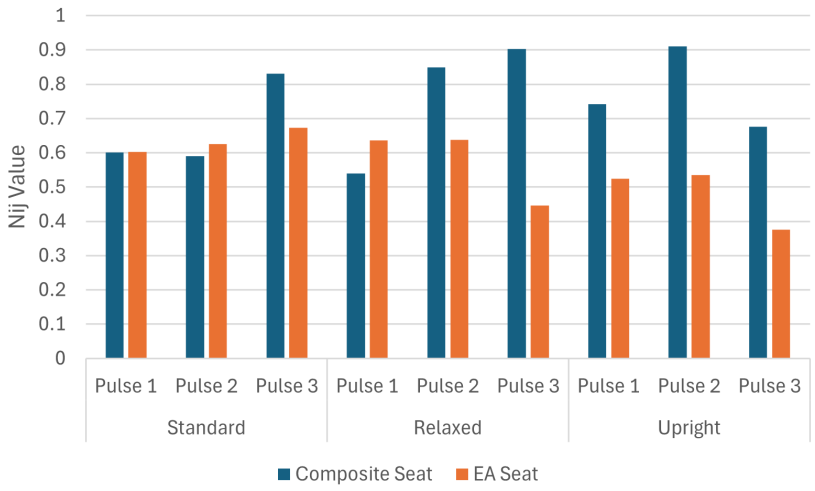

Figure 54 N_{ij} values reported by each occupant model in each test condition

The components resulting in the two highest N_{ij} values varied between the upright and relaxed positions. The 0.91 N_{ij} value reported by the upright position was mainly due to the high bending moment of 50 Nm reported towards the end of the simulation. In contrast, the main contributor to the 0.90 N_{ij} value reported by the relaxed position simulation in the Pulse 3 composite seat test condition was the high levels of tension reported by the model towards the end of the simulation. Evaluating the positions of these models, it is clear that the extension of the head away from the body exhibited by the relaxed position caused this tension force (Figure 56a) and that the bending of the neck caused the reported bending moment in the upright position simulation (Figure 56b).

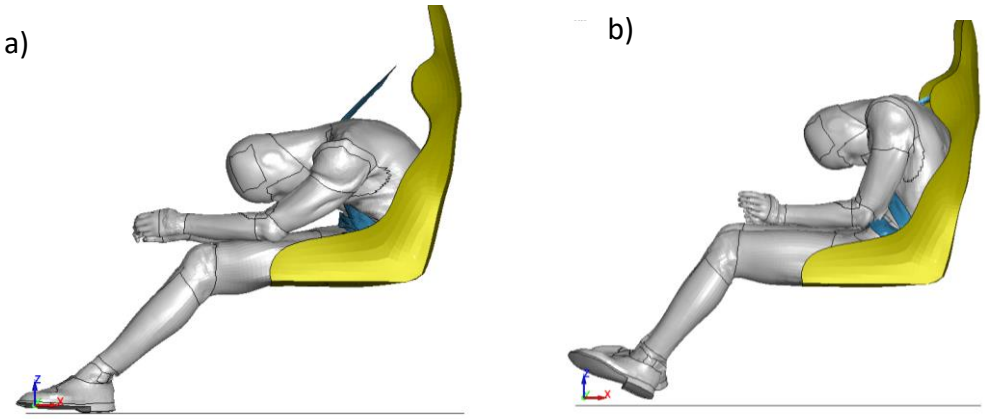

Figure 55 Position of occupant at maximum N_{ij}
a) Relaxed GHBMC pulse 3 composite seat.
b) Upright GHBMC pulse 2 composite seat.

Spinal loading:

All models and test conditions reported similar axial forces associated with each seat utilized (Figure 57). All reported spinal forces for the Composite seat simulations reported values between four and six kgs. In contrast, the EA seat test conditions all reported values between 2.8 and 3.5.

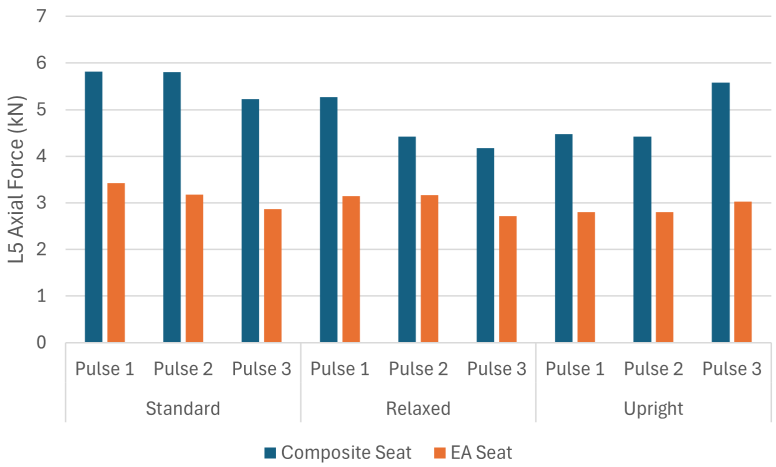

Figure 56 L5 axial forces reported by each occupant model in each test condition.

The lower spinal forces associated with the EA seat remained consistent with previous evaluations. However, the apparent trends related to body position were less consistent in these more realistic simulations. The last study identified a trend of lower spinal loading associated with the relaxed position, which was not apparent in this study. While it is possible that the trend would replicate with more data points, the results from these simulations allude to initial positioning that may not have a considerable effect in crash environments, including horizontal accelerations.

Conclusions:

The primary results from this study were the difficulties presented that necessitated simplification of these simulations. Instabilities were identified in the THOR model, preventing its inclusion in these more complicated models. In addition, computational limitations and instabilities prevented the completion of the full LPC model simulations. These simplified

breakout models appear to be the most advanced environment conditions easily modeled with the current advanced models. Further developments and improvements are possible to run more complex simulation environments. However, these improvements fall outside the scope of this study.

The results reported for the breakout models identified possible mechanisms of occupant injury for head and neck injuries. The potential for head impacts on the occupant's limbs appears most likely with a relaxed-positioned occupant. The relaxed position reported a high-tension force component in the composite seat pulse three conditions. In contrast, the upright position reported a high bending moment in the composite seat pulse two conditions.

To some extent, the spinal loading results agreed with the previous study. While no substantial trends were associated with any GHBMC positions, all models reported a significant reduction in spinal loading in the EA seat. While the EA seat had a varied effect on both head and neck injury metrics, only one case saw a substantially larger injury metric associated with the EA seat. In addition, this one case of increased HIC(Relaxed Pulse 1) value was primarily due to model positioning rather than the seat model implemented.

Chapter 5: Overall Conclusions

Each chapter in this study identified the current capabilities of advanced occupant models and the potential injury risks associated with each crash environment. Chapter 2 recognized a need for further development of the THUMS digital instrumentation for aerospace applications. In addition, the GHBMC model reported sensitivity associated with non-impacting head injuries. Furthermore, there was disagreement between the various occupant models as to the benefits seen from the braced position. In addition, multiple cases identified higher levels of injury risk than measured with the standard ATD models. All these findings should be investigated further to improve aircraft safety. While the presented simulations may need further validation to be used independently of physical testing, the findings identified a need to utilize a combination of approaches to ensure the highest level of safety in aircraft development.

The results and conclusions in chapter 3 further identified results and trends that ATD models and testing alone would not have. Primarily, the ATD models could not evaluate the variable positions as well as the advanced human body models were capable of. The trends of lower injury risk associated with the relaxed position could influence seat manufacturers to research and develop seats designed for this position. In addition, the sensitivity the HBMs reported to the 10g pulse was unseen in the ATD models. Similarly to the F28 testing, these models alone cannot directly influence aircraft design. However, the trends they identified are promising avenues for further research.

Chapter 4 primarily outlines the current limitations of this type of modeling. The difficulties in simulating complex environments were limiting the capabilities of these models. However, the instabilities identified directly outline improvements necessary to expand the potential of this field of study.

Overall, FEM as a tool for crashworthiness investigations must be utilized in conjunction with physical testing. However, through the usage of FEM and advanced HBMs, we can reduce the number of costly physical PMHS tests needed for research. If researchers identify the most likely mechanisms of injury through a combination of tools, future research can prioritize these impact situations for comprehensive PMHS physical testing. This suggested approach would allow for the most extensive investigations of impact scenarios without excessive costs associated with physical PMHS testing. In addition, these further tests would allow for continued model and occupant development, continuing progression toward the ability of FEM to operate independently of physical testing.

Appendix A: Crash Pulses F28 Study

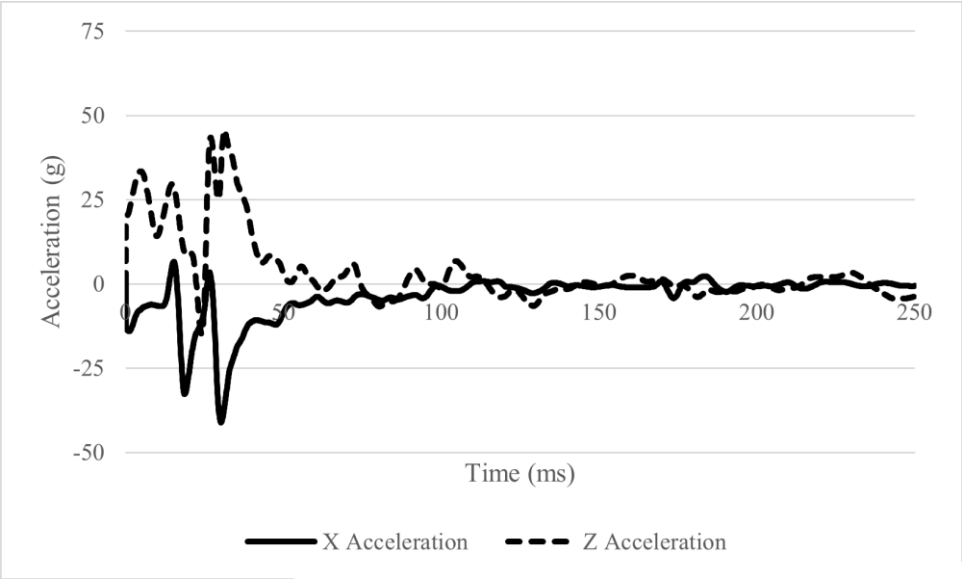

Figure A1. Crash pulse 3A

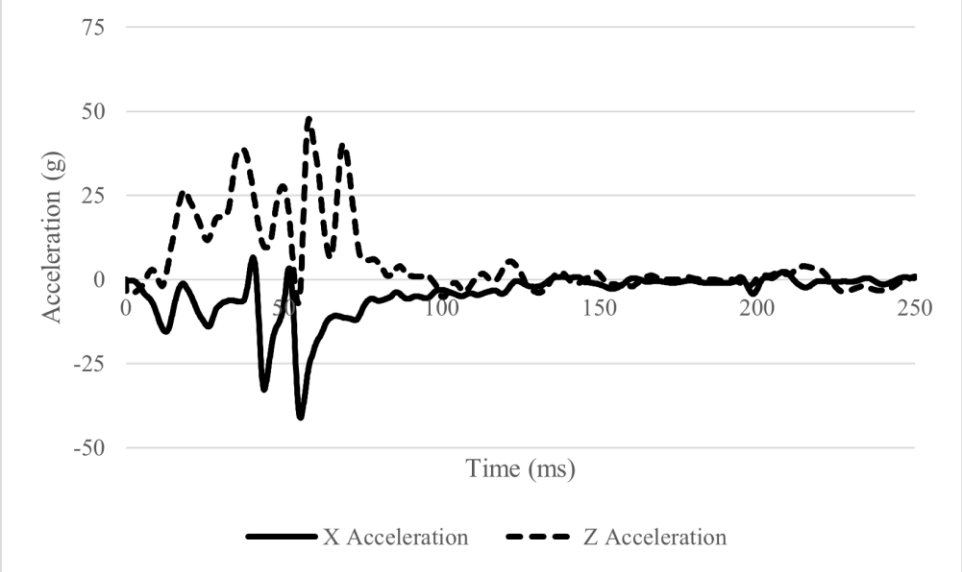

Figure A2. Crash pulse 3D / E

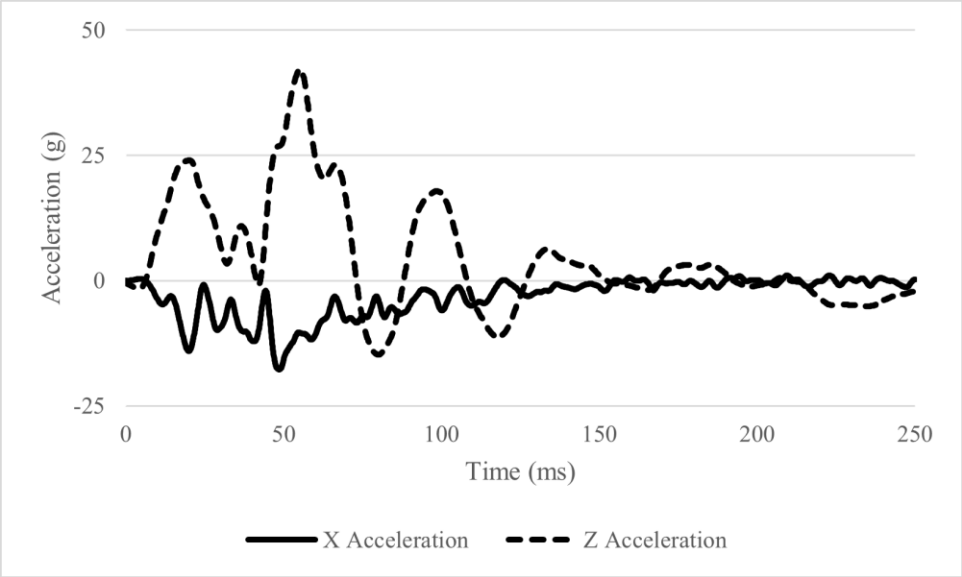

Figure A3. Crash pulse 6A / B

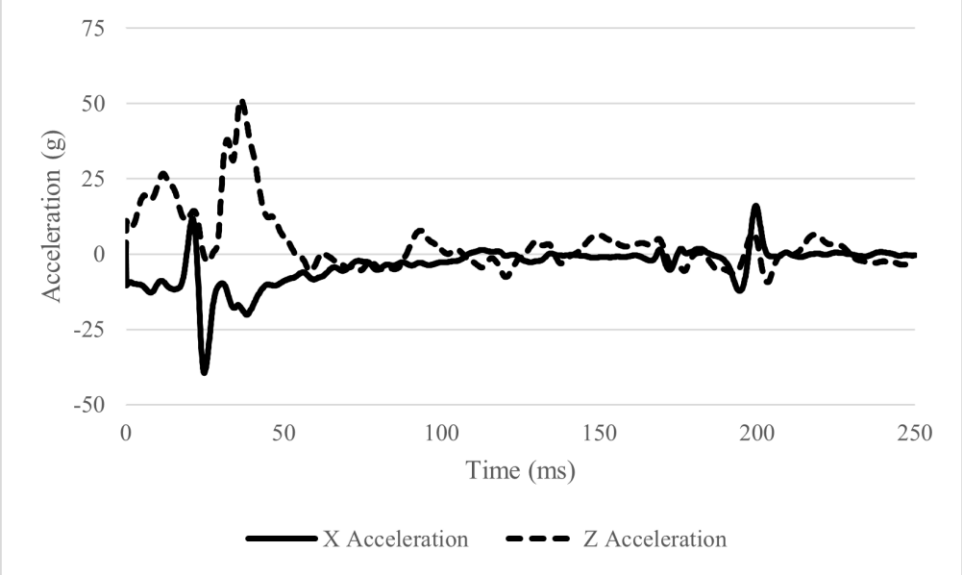

Figure A4. Crash pulse 6D

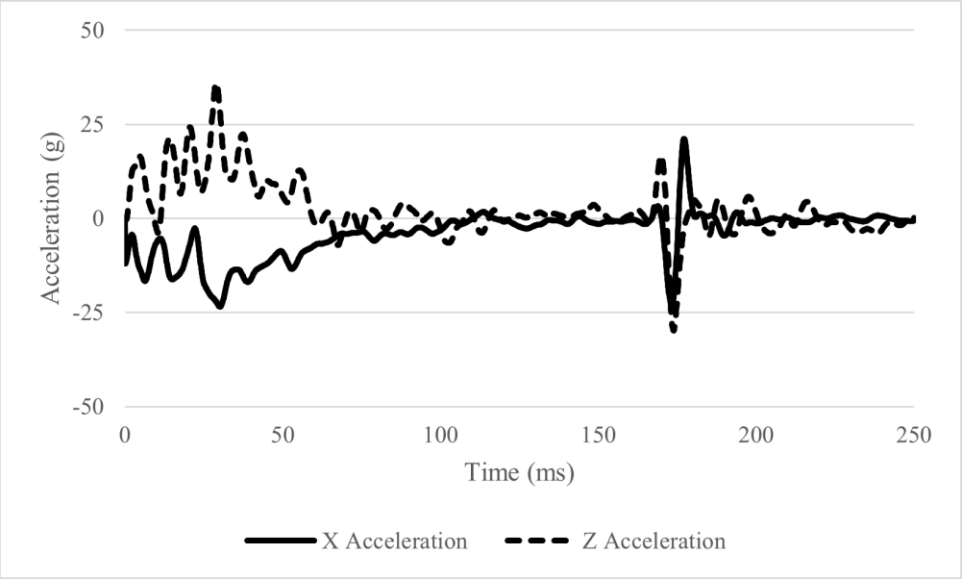

Figure A5. Crash pulse 9D

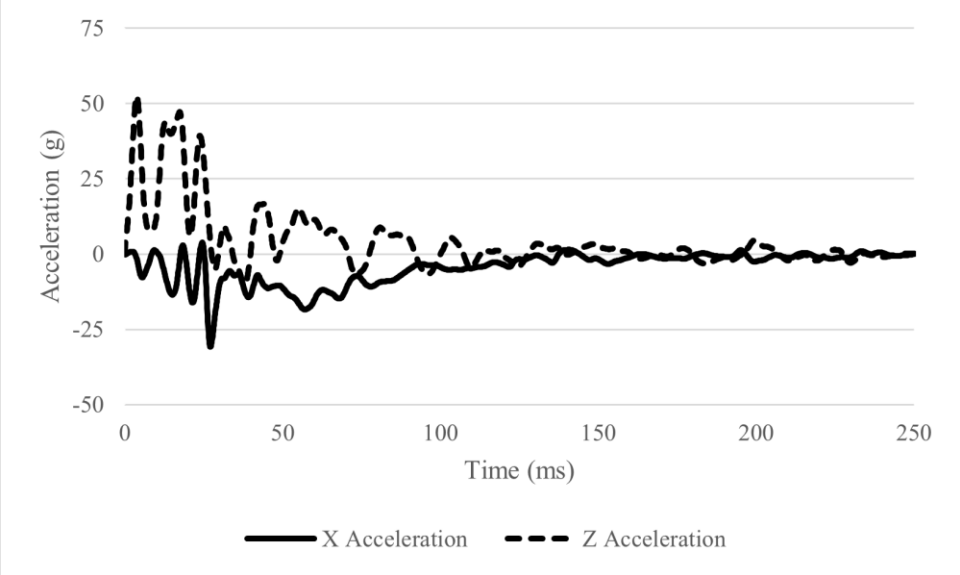

Figure A6. Crash pulse 10C

References:

1. Díaz, J. and M. Costas (2020). Crashworthiness. Encyclopedia of Continuum Mechanics.
2. 14 CFR 25 (2011) Code of federal regulations, title 14, chapter I, subchapter C, part 25 – airworthiness standards: transport category airplanes. Federal Aviation Administration (FAA). United States Department of Transportation (USDOT)
3. Snyder, R., "Crashworthiness Investigation of General Aviation Accidents," SAE Technical Paper 750537, 1975, https://doi.org/10.4271/750537.
4. "Aviation and Plane Crash Statistics | Updated 2024," *Panish | Shea | Ravipudi LLP*, 2024. https://www.panish.law/aviation_accident_statistics.html
5. M. Waimer, T. Feser, P. Schatrow, D. Schueler. Crash concepts for CFRP transport aircraft–comparison of the traditional bend frame concept versus the developments in a tension absorbers concept. Int. J. Crashworthiness, 23 (2) (2018), pp. 193-218
6. X.F. Yang, J.X. Ma, D.S. Wen, J.L. Yang. Crashworthy design and energy absorption mechanisms for helicopter structures: a systematic literatures review Prog. Aero. Sci., 114 (2020), pp. 1-33
7. Haolei Mou, Jiang Xie, Zhenyu Feng, Research status and future development of crashworthiness of civil aircraft fuselage structures: An overview, Progress in Aerospace Sciences, Volume 119, 2020, 100644, ISSN 0376-0421, https://doi.org/10.1016/j.paerosci.2020.100644.
8. "Simulated Crash Testing Saves Time and Money," *Texas A&M Transportation Institute*, Jun. 13, 2013. https://tti.tamu.edu/news/simulated-crash-testing-saves-time-and-money/

9. ANSYS, “What is Finite Element Analysis (FEA)? | Ansys,” *www.ansys.com*. https://www.ansys.com/simulation-topics/what-is-finite-element-analysis
10. K. Jackson and E. Fasanella, “Development of an LS-DYNA Model of an ATR42-300 Aircraft for Crash Simulation.” Accessed: Jan. 16, 2025. [Online]. Available: https://ntrs.nasa.gov/api/citations/20040070893/downloads/20040070893.pdf
11. Foster JK, Kortge JO, Wolanin MJ (1977) Hybrid III. A biomechanically-based crash test dummy. SAE Trans 86:3268–3283
12. V. Gowdy *et al.*, “A Lumbar Spine Modification to the Hybrid III ATD For Aircraft Seat Tests,” *SAE Transactions*, vol. 108, pp. 367–379, 1999, doi: https://doi.org/10.2307/44729421.
13. Bailey, A.M., et al., *Comparison of Hybrid-III and postmortem human surrogate response to simulated underbody blast loading.* J Biomech Eng, 2015. **137**(5): p. 051009.
14. Xu, Lan, et al. “Comparative Performance Evaluation of THOR and Hybrid III.” *SAE Transactions*, vol. 109, 2000, pp. 284–308. *JSTOR*, http://www.jstor.org/stable/44686874. Accessed 16 Jan. 2025.
15. “Wiaman: Diversified Technical Systems,” DTS, https://dtsweb.com/project/wiaman/ (accessed Jan. 16, 2025).
16. Vavalle, N.A., et al., Quantitative Validation of a Human Body Finite Element Model Using Rigid Body Impacts. Annals of Biomedical Engineering, 2015. 43(9): p. 2163-2174.

17. Vikram, A., A. Chawla, and S. Mukherjee, Numerical investigation of THUMS (Total human model for safety) lower extremity FE model for under-body blast loading. Materials Today: Proceedings, 2023. 87: p. 61-66
18. Grindle, D., et al., A validated lower extremity model to investigate the effect of stabilizing knee components in pedestrian collisions. Proc Inst Mech Eng H, 2022. 236(10): p. 1552-1571.
19. Iwamoto, M., et al., *Development of a finite element model of the total human model for safety (THUMS) and application to injury reconstruction.* IRCOBI, 2002: p. 31-42.
20. NASA electric vertical takeoff and landing (VTOL) aircraft technology for public services – a white paper (2021)
21. J. Su, H. Huang, H. Zhang, Y. Wang and F. -Y. Wang, "eVTOL Performance Analysis: A Review From Control Perspectives," in *IEEE Transactions on Intelligent Vehicles*, vol. 9, no. 5, pp. 4877-4889, May 2024, doi: 10.1109/TIV.2024.3387405.
22. N. Swaminathan, S. R. P. Reddy, K. RajaShekara and K. S. Haran, "Flying Cars and eVTOLs—Technology Advancements, Powertrain Architectures, and Design," in *IEEE Transactions on Transportation Electrification*, vol. 8, no. 4, pp. 4105-4117, Dec. 2022, doi: 10.1109/TTE.2022.3172960.
23. Littell, J.D., *A Summary of Airframe Results from a Fokker F28 Full-Scale Crash Test,* N.A.S.A 2020.
24. Putnam, J., *Occupant Response Analysis of a Full-Scale Crash Test of a Fokker F28 Fellowship Aircraft*, N.A.S.A. 2020.

25. Teresa M Reiber, P.C.G., Keegan M Yates, Rachel L Thompson, Aaron M Drake, Nathaniel Newby, Jeffery T Somers, Dustin M Gohmert, Jeffrey D Suhey, Chris E Perry, John R Buhrman, Mark A Baldwin, Cynthia H Null *Comparison of Anthropomorphic Test Device and Human Volunteer Responses in Simulated Landing Impact Tests of U.S. Space Vehicles*, N.A.S.A. 2024.
26. Hostetler, Z.S., et al., *Lower Extremity Validation of a Human Body Model for High Rate Axial Loading in the Underbody Blast Environment.* Stapp Car Crash J, 2022. **66**: p. 99-142.
27. K. Somasundaram, L.Z., D. Sherman, P. Begeman, D. Lyu, J.M. Cavanaugh, *Evaluating thoracolumbar spine response during simulated underbody blast impact using a total human body finite element model.* Journal of the Mechanical Behavior of Biomedical Materials, 2019. **Volume 100**.
28. Karen E. Jackson, J.D.L., Martin S. Annett, and Ian M. Haskin, *Finite Element Simulations of Two Vertical Drop Tests of F-28 Fuselage Sections* -, N.A.S.A.
29. Humanetics, *User's Manual FAA Hybrid III 50th Male Dummy LS-DYNA Model Version*
30. Panzer, M.B., S. Guidice, and D. Parent, *THOR 50th Male Finite Element Model User Manual Model Version 2.1 for LS-Dyna*. 2015.
31. Putnam, J.B., et al., *Development and evaluation of a finite element model of the THOR for occupant protection of spaceflight crewmembers.* Accid Anal Prev, 2015. **82**: p. 244-56.
32. (FAA), F.A.A., *Dynamic Evaluation of Seat Restraint Systems and Occupant Protection on Transport Airplanes*, F.A.A., 2006: Federal Aviation Administration Advisory Circular.

33. International Organization for Standardization., *Road vehicles*. 2013.

34. Barbat, S., et al. *Objective Rating Metric for Dynamic Systems*. in *23rd International Technical Conference on the Enhanced Safety of Vehicles*. 2013. Seoul, South Korea

35. Gayzik, F.S., et al., *Development of a full body CAD dataset for computational modeling: a multi-modality approach.* Ann Biomed Eng, 2011. **39**(10): p. 2568-83.

36. CORPORATION, T.M., *Documentation Total Human Model for Safety (THUMS)*. 2021, TOYOTA CENTRAL R&D LABS., INC.

37. Quanqing Yan, P.H., *Introduction to LS-PrePost*. 2018, LSTC.

38. Eppinger, R., *Development of improved injury criteria for the assessment of advanced automotive restraint systems - II.* N.H.T.S., 2000.

39. "Abbreviated Injury Scale (AIS)," *Association for the Advancement of Automotive Medicine*. https://www.aaam.org/abbreviated-injury-scale-ais-position-statement/

40. Lopez-Valdes, F.J., et al., *Analysis of spinal motion and loads during frontal impacts. Comparison between PMHS and ATD.* Ann Adv Automot Med, 2010. **54**: p. 61-78.

41. Untaroiu, C.D., et al., *A Finite Element Model of a Midsize Male for Simulating Pedestrian Accidents.* J Biomech Eng, 2018. **140**(1).

42. Beillas, P. and F. Berthet, *An investigation of human body model morphing for the assessment of abdomen responses to impact against a population of test subjects.* Traffic Inj Prev, 2017. **18**(sup1): p. S142-S147.

43. DeWit, J.A. and D.S. Cronin, *Cervical spine segment finite element model for traumatic injury prediction.* J Mech Behav Biomed Mater, 2012. **10**: p. 138-50.

44. Mao, H., et al., *Development of a finite element human head model partially validated with thirty five experimental cases.* J Biomech Eng, 2013. **135**(11): p. 111002.
45. Shin, J., N. Yue, and C.D. Untaroiu, *A finite element model of the foot and ankle for automotive impact applications.* Ann Biomed Eng, 2012. **40**(12): p. 2519-31.
46. Yue, N. and C.D. Untaroiu, *A numerical investigation on the variation in hip injury tolerance with occupant posture during frontal collisions.* Traffic Inj Prev, 2014. **15**(5): p. 513-22.
47. Norton, N. *Development of the I-PREDICT Human Body Finite Element Model for Spinal Trauma Prediction in Aviators*. in *SAFE Symposium*. 2023. Virginia Beach, VA.
48. Putnam, J.B., Littell, J.D., Gardner, N., Mennu, M., "Component Characterization of an eVTOL Reference Model for Crashworthiness Studies," Proceedings from the Vertical Flight Society 80th Annual Forum and Technology Display, May 7-9, 2024.
49. Putnam, J. B., Somers, J. T., and Untaroiu, C. D., 2014, "Development, calibration, and validation of a head-neck complex of THOR mod kit finite element model," Traffic Inj Prev, 15(8), pp. 844-854.
50. Brownson, Peter (1993) The brace position for passenger aircraft: a biomechanical evaluation. DM thesis, University of Nottingham.
51. Schwartz, D., Guleyupoglu, B., Koya, B., Stitzel, J. D., and Gayzik, F. S., 2015, "Development of a computationally efficient full human body finite element model," Traffic Inj Prev, 16 Suppl 1, pp. S49-56.

52. Vavalle, N. A., Davis, M. L., Stitzel, J. D., and Gayzik, F. S., 2015, "Quantitative Validation of a Human Body Finite Element Model Using Rigid Body Impacts," Ann Biomed Eng, 43(9), pp. 2163-2174.
53. Jones, N., Untaroiu, C., Putnam, J.B., " Numerical Investigation of Occupant Injury Risks during a Realistic Transport Aircraft Crash Conditions," 61st SAFE Symposium, October 10-12,2023.
54. "KINETICS tool of ANSA for Multi Body Dynamics." Accessed: Oct. 28, 2024. [Online]. Available: https://www.beta-cae.com/pdf/ansa_kinematics_tool.pdf
55. Kwong Ming Tse, Dale Lee Robinson, Melanie Franklyn, Jiang Yue Zhang, E. Meade Spratley, Robert Scott Salzar, Justin Fernandez, David Charles Ackland, Peter Vee Sin Lee,"Effect of sitting posture on pelvic injury risk under vertical loading", Journal of the Mechanical Behavior of Biomedical Materials, Volume 108, 2020, 103780, ISSN 1751-6161, https://doi.org/10.1016/j.jmbbm.2020.103780.
56. Federal Aviation Administration. "Emergency Landing Dynamic Conditions." 14 CFR § 23.562. Amended December 2, 2011.
57. Federal Aviation Administration, "Emergency Landing Dynamic Conditions," 14 CFR § 27.561, Amended November 13, 1989.
58. Littell, J.D., "Full-Scale Crash Test of an MD-500 Helicopter," Proceedings from the American Helicopter Society 67th Annual Forum, May 3-5, 2011

59. Littell, J.D., Putnam, J.B., “A Summary of Test Results from a NASA Lift + Cruise eVTOL Crash Test,” Proceedings from the Vertical Flight Society 79th Annual Forum and Technology Display, May 16-18, 2023.
60. Guha, S. "LSTC_NCAC Hybrid III 50th Dummy Positioning & Post-Processing," Livermore Software Technology Corporations. 2014.
61. Thunert, C. “CORAplus Release 4.0.4 User’s Manual,” Partnership for Dummy Technology and Biomechanics. May 2017.
62. International Organization for Standardization. "Road vehicles." ISO/TS 18571. 2014.
63. M. Reed and S. Ebert, “THE SEATED SOLDIER STUDY: POSTURE AND BODY SHAPE IN VEHICLE SEATS,” 2013. Accessed: Oct. 28, 2024. [Online]. Available: https://deepblue.lib.umich.edu/bitstream/handle/2027.42/109725/103143.pdf?sequence=1&isAllowed=y
64. Hodgson, V. R. and L. M. Thomas (1972). “Effect of long-duration impact on head.” Society of Automotive Engineers SAE 720956.
65. Prasad, P. and R. P. Daniel (1984). “A biomechanical analysis of head, neck, and torso injuries to child surrogates due to sudden torso acceleration.” SAE TRANSACTIONS: 784-79.
66. Yoganandan N., et al., Human lumbar spinal column injury criteria from vertical loading at the base: Applications to military environments J Mech Behav Biomed Mater. 2020